Summer 6-12-2017

Structurally Diverse Boron-Nitrogen Heterocycles from an N2O23– Formazanate Ligand

Stephanie M. Barbon
sbarbon@uwo.ca

Viktor N. Staroverov
vstarove@uwo.ca

Joe Gilroy
jgilroy5@uwo.ca

Structurally Diverse Boron-Nitrogen Heterocycles from an $N_2O_2^{3-}$ Formazanate Ligand

Stephanie M. Barbon,[a] Viktor N. Staroverov,[a] and Joe B. Gilroy*[a]

Abstract: Five new compounds comprised of unprecedented boron-nitrogen heterocycles have been isolated from a single reaction of a potentially tetradentate $N_2O_2^{3-}$ formazanate ligand with BF_3•OEt_2 and NEt_3. Optimized yields for each product were obtained through variation of experimental conditions and rationalized in terms of relative Gibbs free energies of the products as determined by electronic structure calculations. Chemical reduction of two of these compounds resulted in the formation of a stable anion, radical anion, and diradical dianion. Structural and electronic properties of this new family of redox-active heterocycles were characterized using UV-vis absorption spectroscopy, cyclic voltammetry and X-ray crystallography.

Boron-nitrogen (BN) heterocycles are of significant interest to a wide range of disciplines on account of their unusual structure, bonding, and properties.[1-3] The most common compounds containing such heterocycles, azaborines, find applications in organic electronics and chemical hydrogen storage.[4-6] Other BN heterocycles, exemplified by compounds **1**–**6**, are noted for their unexpected reactivity and, in many cases, unique redox properties.[7-16]

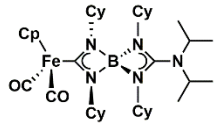

1 (Aldridge)

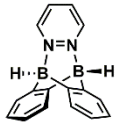

2 (Wagner)

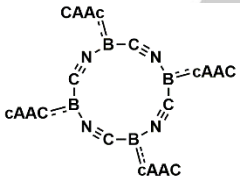

3 (Braunschweig)

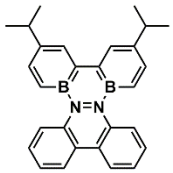

4 (Piers)

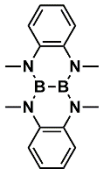

5 (Russell)

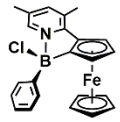

6 (Jäkle)

Each of compounds **1**–**3** contains BN bonds in an unusual framework.[17-19] Piers' B_2N_2 triphenylene analogue **4** can be reduced to form a stable radical anion,[20] and Russell's polycyclic borazine **5** undergoes oxidation to form a stable radical cation.[21] The Jäkle group has demonstrated that ferrocene-boron compound **6** can be converted to a planar borenium cation via abstraction of the chloride.[22]

[a] S. M. Barbon, Prof. Dr. V. N. Staroverov, Prof. Dr. J. B. Gilroy
Department of Chemistry and The Centre for Advanced Materials and Biomaterials Research (CAMBR)
The University of Western Ontario
1151 Richmond St. N., London, ON, Canada, N6A 5B7
E-mail: joe.gilroy@uwo.ca

Supporting information for this article is given via a link at the end of the document.

Our group is interested in boron complexes of formazanate ligands.[23] Boron difluoride adducts of these ligands have many fascinating and useful properties, including high molar absorptivities and a capacity for reversible stepwise reduction.[24-25] In this work, we set out to study the properties of similar compounds derived from trianionic, potentially tetradentate formazanate ligands.

The parent formazan **7** was synthesized according to a published method.[26] Upon reaction of **7** with BF_3•OEt_2 in the presence of NEt_3 followed by the addition of H_2O (Scheme 1), the expected product **8** was not detected; instead, the reaction mixture was found to contain formazan **7** and five new compounds (**9**–**13**), which could be separated by column chromatography in typical combined yields of 65–75% (Figure S1). Careful analysis of ^{1}H, ^{11}B, ^{13}C and ^{19}F NMR spectra, and single-crystal X-ray diffraction analysis enabled us to identify all six compounds present (Figures 1, 2, S2–S12). The complex reaction mixture obtained was in striking contrast to the clean conversion of formazan **14** to boron compound **15** in 92% yield under identical conditions (Scheme 1, Figures S13–S17).

To rationalize these observations, we used density-functional methods to calculate the changes in standard thermodynamic state functions for the reaction pathways leading from **7** to **8**–**13** and from **14** to **15** under the experimental reaction conditions (80 °C, 1 atm, toluene solution). The calculations were performed with the *Gaussian 09* program[27] using the hybrid version of the Perdew-Burke-Ernzerhof density functional[28] (PBE1PBE), the 6-311+G(d,p) basis set, and implicit solvation methods (Table S5). According to this level of theory, the formation of tetradentate boron compound **8** from **7** is thermodynamically unfavourable ($\Delta G°$ = 75.7 kJ mol^{-1}), whereas the formation of tetradentate compound **15** from **14** is favourable ($\Delta G°$ = −19.4 kJ mol^{-1}). It appears that the 5-membered chelates of **8** are too strained to form, so less strained compounds are produced instead. Compound **13**, the most abundant product which appears to form *via* **12**, was predicted to be decidedly favoured ($\Delta G°$ = −68.6 kJ mol^{-1}).

Through variation of reaction conditions, we optimized the yields of each of the five new compounds produced (Table S4). When elevated temperatures or longer reaction times were employed, the ratio of **13** to **9** and **10** was increased. When greater excess amounts of BF_3•OEt_2 and NEt_3 were used, products **9** and **10** were obtained in higher yields.

The six compounds present in the reaction mixture were separated by column chromatography (CH_2Cl_2, silica gel). The first two that eluted (R_f = 0.82, 0.76) yielded similar NMR spectra without ^{19}F resonances. We identified these compounds using X-ray crystallography as dimers **9** and **10** (Figure 1a, b). Both structures contain a ten-membered ring (-B-O-C-C-N-B-O-C-C-N-), where B–O bonds bridge the monomeric units. The difference between the two structures is the orientation of the ten-membered ring, a *pseudo*-chair conformation in compound **9** and a *pseudo*-boat conformation in compound **10** (see insets, Figure 1a, b). We did not observe interconversion between these two products in solution, even upon prolonged heating.

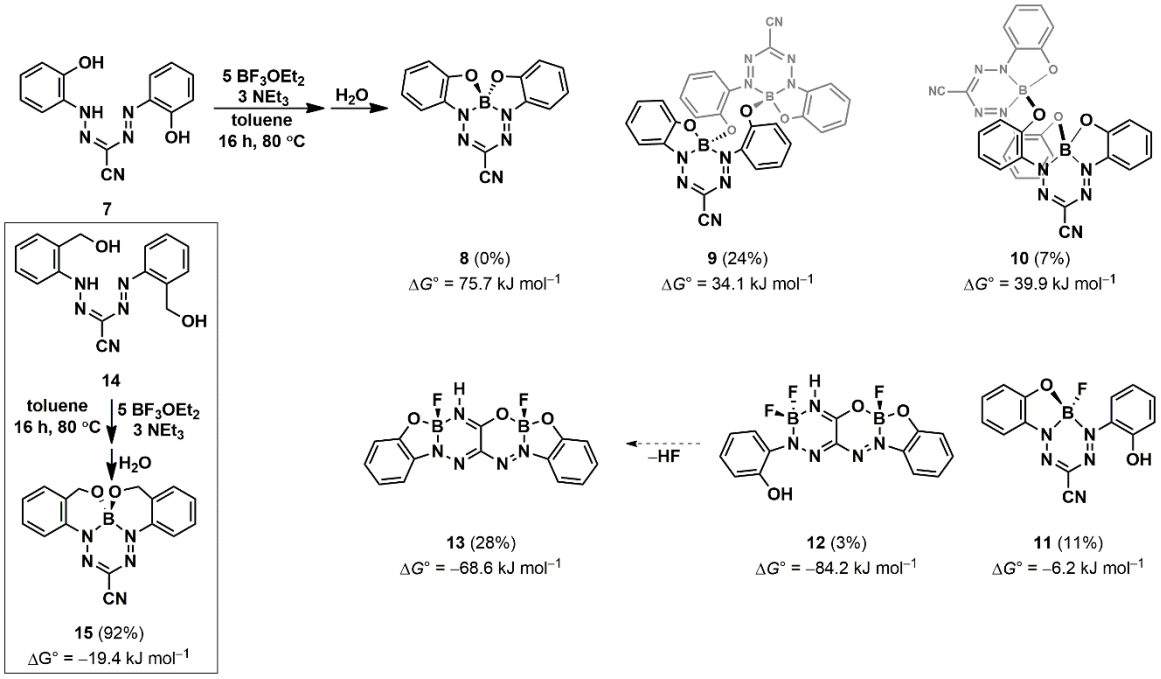

Scheme 1. Products formed from the reaction of formazan **7** with BF_3•OEt_2 and NEt_3. The inset indicates the product formed from the reaction of formazan **14** with BF_3•OEt_2 and NEt_3. The Gibbs free energies ($\Delta G°$) were computed for the formation of each compound from the corresponding formazan and the stoichiometric number of BF_3 and H_2O molecules under conditions simulating those employed in the actual synthesis, and are expressed in kJ mol^{-1} of the formazan. The dashed arrow indicates interconversion in solution.

The *pseudo*-boat conformation leads to a π-stacking interaction between aryl substituents and the formazanate backbone in the solid-state phase of **10**, which is not observed in **9**. In solution, this interaction causes broadening of the low-energy absorption of **10** and the appearance of a shoulder at 597 nm that is not present in the absorption profile of **9** (Figures 1e, S18, Table S1).

The cyclic voltammograms (CVs) of compounds **9** and **10** included three reduction waves (Figure 1f, Table S1). Both compounds exhibit two reversible one-electron reduction waves (**9**: E_{red1} = −760 mV, E_{red2} = −1010 mV; **10**: E_{red1} = −720 mV, E_{red2} = −1020 mV), and a third irreversible two-electron reduction (**9**: E_{onset} = −1730 mV; **10**: E_{onset} = −1770 mV). The reversible waves correspond to the stepwise reduction of the formazanate backbones to *mono*- and *bis*-radical anions and the irreversible wave to the formation of *bis*-dianions. The difference between the reversible reduction potentials (ΔE_{red}) was 250 mV for **9** and 290 mV for **10**.

Compound **10** proved easier to isolate than its structural isomer **9**, so it was chosen for further reactivity studies. Reduction with one and two equivalents of cobaltocene yielded compounds $\mathbf{10}^{\bullet-}$ and $\mathbf{10}^{\bullet 2-}$, both of which produced broad isotropic EPR spectra at g = 2.0038 (Figure S19). Both species were characterized by single-crystal X-ray diffraction analysis (Figure 1c, d, Table S2). The average N–N bond length in the neutral dimer **10** was 1.314(3) Å, which is typical of an N–N bond with a bond order of ~1.5. In compound $\mathbf{10}^{\bullet-}$, the average N–N bond length for N1 to N4 is 1.360(3) Å, suggesting the presence of a borataverdazyl radical in which the additional electron occupies an orbital with antibonding N–N character.[24, 29-30] The average N–N bond length for N5 to N8 is 1.315(3) Å, typical of a formazanate adduct.[24] These metrics confirm that chemical reduction occurs in a stepwise fashion and that the radical anion is localized on one formazanate ligand. In the doubly reduced species $\mathbf{10}^{\bullet 2-}$, the average N–N bond length was 1.366(3) Å, which corresponds to N–N single bonds as expected for borataverdazyl radicals.[30] These conclusions were corroborated by UV-vis absorption spectroscopy in CH_3CN (Figure 1e, Table S1). Neutral dimer **10** has a λ_{max} at 569 nm and a molar absorptivity (ε) of 20 500 M^{-1} cm^{-1}. Singly reduced $\mathbf{10}^{\bullet-}$ absorbs strongly at 568 nm, as well as 687 and 477 nm, which is typical of verdazyl species[30] and shows that $\mathbf{10}^{\bullet-}$ is made up of independent borataverdazyl and formazanate units. Doubly reduced species $\mathbf{10}^{\bullet 2-}$ absorbs minimally at 568 nm, but exhibits two absorption peaks typical of borataverdazyl anions with λ_{max} of 687 nm (ε = 8 200 M^{-1} cm^{-1}) and 477 nm (ε = 39 200 M^{-1} cm^{-1}).[31]

We were unable to grow single crystals of the third compound to elute (R_f = 0.61). However, using ^{1}H, ^{11}B, ^{13}C and ^{19}F NMR spectroscopy and mass spectrometry, we identified it as **11**. This product is dark blue, can be reversibly reduced twice (Figures S20, S21, Table S1), and slowly converts to formazan **7** in solution. The fourth compound that eluted from the column (R_f = 0.39) was formazan **7**, present as a result of incomplete reactivity or hydrolysis of unstable, unidentified species formed during the reaction.

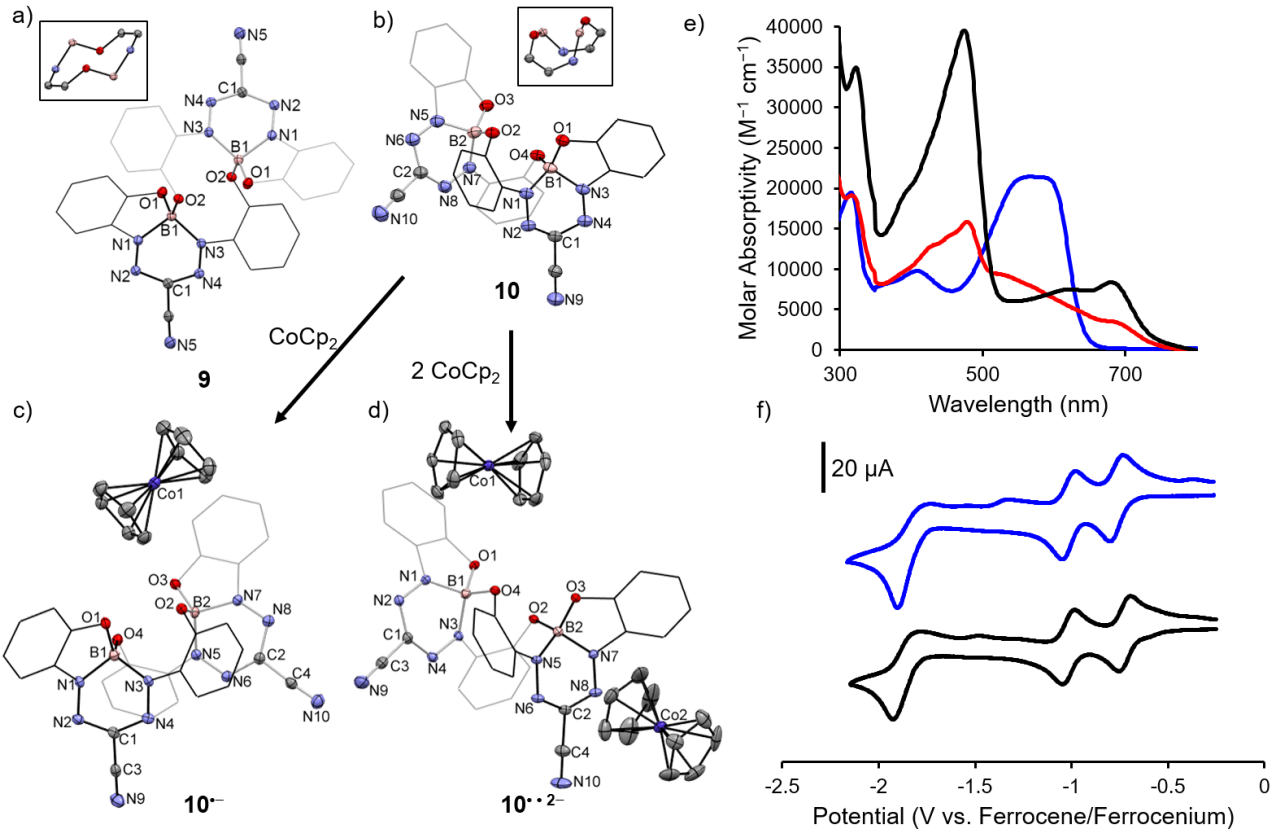

Figure 1. Solid-state structures of (a) **9**, (b) **10**, (c) **10**$^{\bullet-}$ and (d) **10**$^{\bullet\bullet 2-}$. Thermal displacement ellipsoids are shown at the 50% probability level. Phenyl substituents are wireframe and hydrogen atoms are removed for clarity. Arrows indicate conditions for the formation of **10**$^{-}$ and **10**$^{\bullet\bullet 2-}$. Insets in panels (a) and (b) show only the atoms in the respective ten-membered rings. Panel (e) shows UV-vis absorption spectra of compounds **10** (blue), **10**$^{\bullet-}$ (red) and **10**$^{\bullet\bullet 2-}$ (black) in CH_3CN. Panel (f) shows CVs of **9** (black) and **10** (blue) recorded at 100 mV s^{-1} in 1 mM CH_2Cl_2 solutions containing 0.1 M [nBu$_4$N][PF$_6$] as supporting electrolyte.

The final two compounds that eluted from the column (R_f = 0.31, 0.22) were identified as **12** and **13**. Interestingly, **13** showed two doublets in its ^{11}B NMR spectrum due to the coupling of each boron atom with a single fluorine atom ($^1J_{BF}$ = 33, 42 Hz). Single-crystal X-ray diffraction analysis confirmed that compound **13** was not a dimer, but contained two boron atoms bonded to one formazanate ligand, where the cyano group had been hydrolyzed.[32] Compound **12** is similar to **13** aside from a free OH group and a BF_2 unit. In solution, **12** converts to **13** over the course of a few hours. The λ_{max} of **12** is blue-shifted by 17 nm in CH_2Cl_2 with respect to **13** (Figure S22, S23). Compound **13** yielded a single reversible one-electron reduction in its CV (Figure S24), prompting us to perform chemical reduction using one equivalent of cobaltocene. The solution changed from pink-purple to dark blue-purple (Figure 2a). Attempts to crystallize the resulting compounds were unsuccessful, so a salt metathesis reaction was performed with [nBu$_4$N][Br] in order to exchange the cobaltocenium cation for the solubilizing tetra-*n*-butyl ammonium cation. The colour of the solution was unchanged throughout this process. Single-crystal X-ray diffraction revealed the resulting product to be anion **16**$^{-}$. Upon reduction, the NH bond in **13** appears to cleave homolytically, resulting in the formation of **16**$^{-}$ and H_2 (Figure 2c). The proposed structure was confirmed by ^{1}H and ^{13}C NMR spectroscopy, mass spectrometry and IR spectroscopy (see Figure S25, S26). Aside from the loss of the *N*-bonded proton, the connectivity in **16**$^{-}$ is identical to that of **13** (Figures 2b, c). The B1-N5 bond has shortened (**13**: 1.516(3) Å; **16**$^{-}$: 1.442(5) Å) and the C2-N5 bond has lengthened (**13**: 1.304(3) Å; **16**$^{-}$: 1.327(4) Å, Table 3). The angles around B1 and N5 change with the presence of the lone pair. For example, the N1-B1-N5 angle widens by ~3.5°, while the B1-N5-C2 angle contracts by ~3.6°. The same angles around B2 change less drastically (N3-B2-O2 angle contracts by 1.1°, and the B2-O3-C2 angle contracts by 2.0°). **16**$^{-}$ is highly absorbing (ε = 18 000 M^{-1} cm^{-1}), with a low-energy λ_{max} of 589 nm that was red-shifted by 12 nm with respect to neutral **13** (Figures S23, S27).

The calculated highest occupied molecular orbitals (HOMO) of **13** and **16**$^{-}$ are delocalized over the entire molecules (Figure 2d). The lowest unoccupied molecular orbitals (LUMO) were delocalized over the formazanate nitrogen atoms and the *N*-aryl substituents. Time-dependent PBE1PBE/6-311+G(d,p) calculations for **13** and **16**$^{-}$ in CH_2Cl_2 solution showed the HOMO and LUMO to be the dominant orbital pair involved in the lowest-energy electronic excitation in both molecules, and approximately reproduced the shift in λ_{max} from **13** to **16**$^{-}$ ($\Delta\lambda_{calc}$ = 8 nm, $\Delta\lambda_{obs}$ = 12 nm, Table S6).

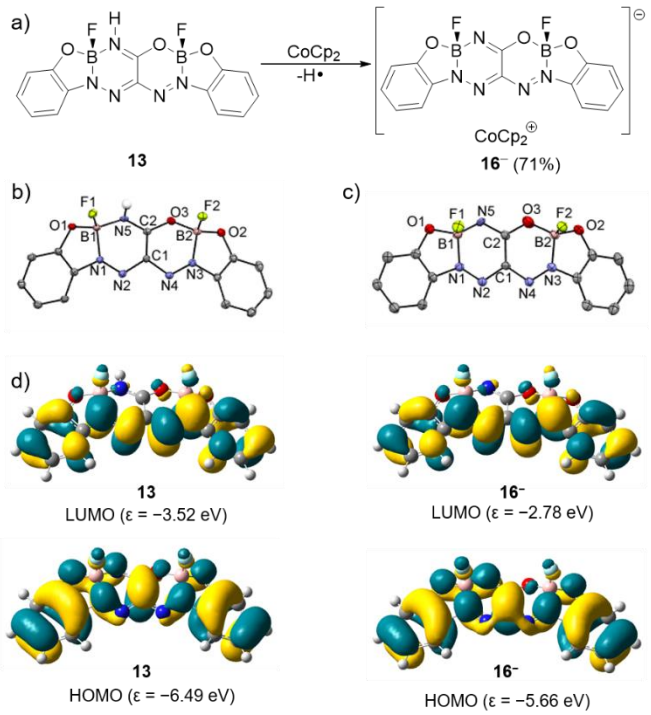

Figure 2. (a) Chemical reduction of **13** to **16**$^-$ with cobaltocene. Solid-state structures of (b) **13** and (c) **16**$^-$ with thermal displacement ellipsoids shown at the 50% probability level. Hydrogens, aside from the hydrogen on N5 in **13**, and the *n*Bu_4N cation in **16**$^-$ have been removed for clarity. (d) HOMOs and LUMOs for **13** and **16**$^-$ calculated at the PBE1PBE/6-311+G(d,p) level.

In conclusion, we have reported the synthesis of five new BN heterocycles **9**–**13** by one straightforward reaction, starting from an $N_2O_2^{3-}$ formazanate ligand. The observed product distribution appears to be strain-driven as evidenced by the fact that similar heterocycles were not formed when the reactant **7** was replaced by a homologous compound **14**. Each of compounds **9**–**13** exhibited interesting optical and electrochemical properties. In particular, compound **10** was reduced to stable *mono*- and *bis*-radical anions with electronically-isolated formazanate/verdazyl units. Compound **13**, which contains an unprecedented BN core, could be readily converted into stable anion **16**$^-$. This study will form a platform for the rational design of novel BN heterocycles with potential utility as light-harvesting and charge-transporting materials in the future.

Acknowledgements

This work was supported by the Natural Science and Engineering Research Council (NSERC) of Canada (J. B. G.: DG RGPIN-2013-435675, V. N. S.: DG RGPIN-2015-04814 and S. M. B.: CGS D scholarship), the Ontario Ministry of Research and Innovation (J. B. G.: ERA, ER-14-10-147) and the Canadian Foundation for Innovation (J. B. G.: JELF 33977).

Keywords: BN Heterocycles • Formazanate Ligands • Redox Chemistry • Boron Chemistry • Stable Radicals

[1] M. J. D. Bosdet and W. E. Piers, *Can. J. Chem.*, **2009**, *87*, 8–29.
[2] K. Ma, M. Scheibitz, S. Scholz and M. Wagner, *J. Organomet. Chem.*, **2002**, *652*, 11–19.
[3] J. Brand, H. Braunschweig and S. S. Sen, *Acc. Chem. Res.*, **2014**, *47*, 180–191.
[4] P. G. Campbell, A. J. V. Marwitz and S.-Y. Liu, *Angew. Chem. Int. Ed.*, **2012**, *51*, 6074–6092.
[5] P. G. Campbell, L. N. Zakharov, D. J. Grant, D. A. Dixon and S.-Y. Liu, *J. Am. Chem. Soc.*, **2010**, *132*, 3289–3291.
[6] X.-Y. Wang, H.-R. Lin, T. Lei, D.-C. Yang, F.-D. Zhuang, J.-Y. Wang, S.-C. Yuan and J. Pei, *Angew. Chem. Int. Ed.*, **2013**, *52*, 3117–3120.
[7] J. S. A. Ishibashi, J. L. Marshall, A. Mazière, G. J. Lovinger, B. Li, L. N. Zakharov, A. Dargelos, A. Graciaa, A. Chrostowska and S.-Y. Liu, *J. Am. Chem. Soc.*, **2014**, *136*, 15414–15421.
[8] H. Braunschweig, W. C. Ewing, K. Geetharani and M. Schäfer, *Angew. Chem. Int. Ed.*, **2015**, *54*, 1662–1665.
[9] D.-T. Yang, S. K. Mellerup, J.-B. Peng, X. Wang, Q.-S. Li and S. Wang, *J. Am. Chem. Soc.*, **2016**, *138*, 11513–11516.
[10] O. Dilek, Z. Lei, K. Mukherjee and S. Bane, *Chem. Commun.*, **2015**, *51*, 16992–16995.
[11] H. Braunschweig, T. Herbst, D. Rais, S. Ghosh, T. Kupfer, K. Radacki, A. G. Crawford, R. M. Ward, T. B. Marder, I. Fernández and G. Frenking, *J. Am. Chem. Soc.*, **2009**, *131*, 8989–8999.
[12] S. Pietsch, U. Paul, I. A. Cade, M. J. Ingleson, U. Radius and T. B. Marder, *Chem. Eur. J.*, **2015**, *21*, 9018–9021.
[13] A. W. Baggett, F. Guo, B. Li, S.-Y. Liu and F. Jäkle, *Angew. Chem. Int. Ed.*, **2015**, *54*, 11191–11195.
[14] H. Noda, M. Furutachi, Y. Asada, M. Shibasaki and N. Kumagai, *Nat. Chem.*, **2017**, DOI: 10.1038/nchem.2708.
[15] H. Helten, *Chem. Eur. J.*, **2016**, *22*, 12972–12982.
[16] M.-C. Chang and E. Otten, *Inorg. Chem.*, **2015**, *54*, 8656–8664.
[17] G. A. Pierce, S. Aldridge, C. Jones, T. Gans-Eichler, A. Stasch, N. D. Coombs and D. J. Willock, *Angew. Chem. Int. Ed.*, **2007**, *46*, 2043–2046.
[18] A. Lorbach, M. Bolte, H.-W. Lerner and M. Wagner, *Chem. Commun.*, **2010**, *46*, 3592–3594.
[19] M. Arrowsmith, D. Auerhammer, R. Bertermann, H. Braunschweig, G. Bringmann, M. A. Celik, R. D. Dewhurst, M. Finze, M. Grüne, M. Hailmann, T. Hertle and I. Krummenacher, *Angew. Chem. Int. Ed.*, **2016**, *55*, 14464–14468.
[20] C. A. Jaska, D. J. H. Emslie, M. J. D. Bosdet, W. E. Piers, T. S. Sorensen and M. Parvez, *J. Am. Chem. Soc.*, **2006**, *128*, 10885–10896.
[21] X. Xie, C. J. Adams, M. A. M. Al-Ibadi, J. E. McGrady, N. C. Norman and C. A. Russell, *Chem. Commun.*, **2013**, *49*, 10364–10366.
[22] J. Chen, R. A. Lalancette and F. Jäkle, *Chem. Commun.*, **2013**, *49*, 4893–4895.
[23] A. W. Nineham, *Chem. Rev.*, **1955**, *55*, 355–483.
[24] S. M. Barbon, P. A. Reinkeluers, J. T. Price, V. N. Staroverov and J. B. Gilroy, *Chem. Eur. J.*, **2014**, *20*, 11340–11344.
[25] M.-C. Chang and E. Otten, *Chem. Commun.*, **2014**, *50*, 7431–7433.
[26] J. B. Gilroy, P. O. Otieno, M. J. Ferguson, R. McDonald and R. G. Hicks, *Inorg. Chem.*, **2008**, *47*, 1279–1286.
[27] M. J. Frisch, G. W. Trucks, H. B. Schlegel *et al.*, Gaussian 09, Revision E.01 (Gaussian, Inc., Wallingford CT, 2013).
[28] M. Ernzerhof and G. E. Scuseria, *J. Chem. Phys.*, **1999**, *110*, 5029–5036.
[29] J. B. Gilroy, M. J. Ferguson, R. McDonald, B. O. Patrick and R. G. Hicks, *Chem. Commun.*, **2007**, 126–128.
[30] M.-C. Chang, A. Chantzis, D. Jacquemin and E. Otten, *Dalton Trans.*, **2016**, *45*, 9477–9484.
[31] The contribution from cobaltocenium is assumed to be negligible above 300 nm. See N. El Murr, *J. Organomet. Chem.*, **1976**, *112*, 189–199.
[32] Quenching the reaction with ammonia did not afford the symmetric analog of **13**.

Entry for the Table of Contents

COMMUNICATION

Five novel boron-nitrogen heterocycles based on an $N_2O_2^{3-}$ formazanate ligand have been isolated as unexpected products of a single reaction. The reduction of two of these heterocycles yielded an unusual anion, radical anion, and diradical dianion.

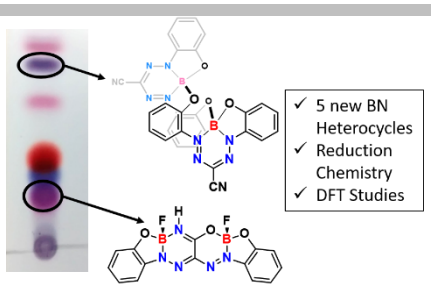

*S. M. Barbon, V. N. Staroverov, J. B. Gilroy**

Page No. – Page No.

Structurally Diverse Boron-Nitrogen Heterocycles from an $N_2O_2^{3-}$ Formazanate Ligand

Table of Contents

Table S1. Optical and electronic properties of complexes **9**−**13** and their reduction products.

	Solvent	λ_{max} (nm)	E (M^{-1} cm^{-1})	E_{red1} (mV)	E_{red2} (mV)	E_{red3} (mV)	E_{ox1} (mV)
9	CH_2Cl_2	535	28 100	−760	−1010	−1730[a]	1060[a]
10	CH_2Cl_2	569	20 500	−720	−1020	−1770[a]	1020[a]
11	CH_2Cl_2	577	13 500	−720	−1630	–	606[a]
12	CH_2Cl_2	560	27 600	–	–	–	–
13	CH_2Cl_2	577	35 900	−770	−1130[a]	–	839[a]
$10^{\bullet-}$	CH_3CN	477	15 500	–	–	–	–
$10^{\bullet\bullet 2-}$	CH_3CN	477	39 200	–	–	–	–
16^-	CH_2Cl_2	589	18 000	–	–	–	–

[a]Onset of irreversible reduction or oxidation.

Experimental Section

General considerations

Reactions and manipulations were carried out under a nitrogen atmosphere using standard Schlenk techniques unless otherwise stated. Solvents were obtained from Caledon Laboratories, dried using an Innovative Technologies Inc. solvent purification system, collected under vacuum and stored under a nitrogen atmosphere over 4 Å molecular sieves. Reagents were purchased from Sigma-Aldrich or Alfa Aesar and used as received. Formazan **7** was prepared according to a literature procedure.[1]

NMR spectra were recorded on 400 MHz (^{1}H: 399.8 MHz, ^{11}B: 128.3 MHz, ^{19}F: 376.1 MHz) or 600 MHz (^{1}H: 599.5 MHz, ^{13}C: 150.8 MHz) Varian INOVA instruments. ^{1}H NMR spectra were referenced to residual $CHCl_3$ (7.26 ppm), $CHDCl_2$ (5.32 ppm) or DMSO-d_5 (2.50 ppm) and $^{13}C\{^1H\}$ NMR spectra were referenced to $CDCl_3$ (77.2 ppm), CD_2Cl_2 (53.8 ppm), or DMSO-d_6 (39.5 ppm). ^{11}B spectra were referenced to $BF_3{\cdot}OEt_2$ at 0 ppm and ^{19}F spectra were referenced to $CFCl_3$ at 0 ppm. Mass spectrometry data were recorded in positive-ion mode using a high-resolution Finnigan MAT 8200 spectrometer using electron impact ionization. UV-vis absorption spectra were recorded using a Cary 5000 instrument. Four separate concentrations were run for each sample and molar extinction coefficients were determined from the slope of a

plot of absorbance against concentration. FT-IR spectra were recorded using an attenuated total reflectance (ATR) attachment using a Bruker Vector 33 FT-IR spectrometer. Elemental analyses (C, H, N) were carried out by Laboratoire d'Analyse Élémentaire de l'Université de Montréal, Montréal, QC, Canada or Canadian Microanalytical Services Ltd., Delta, BC, Canada.

Purity of new compounds

The purity of diamagnetic compounds described in this study was demonstrated by providing very clean ^{1}H, ^{11}B, $^{13}C\{^{1}H\}$, and ^{19}F NMR spectra and high resolution mass spectrometry data. For paramagnetic compounds $\mathbf{10}^{\bullet-}$ and $\mathbf{10}^{\bullet\bullet 2-}$, carbon analysis was consistently low, while H and N analysis matched well across several independent batches, due to the presence of boron, which often hampers C analysis.[2],[3] However, these data are provided to illustrate the best values obtained to date.

Electrochemical methods

Cyclic voltammetry experiments were performed with a Bioanalytical Systems Inc. (BASi) Epsilon potentiostat and analyzed using BASi Epsilon software. Electrochemical cells consisted of a three-electrode setup including a glassy carbon working electrode, platinum wire counter electrode and silver wire *pseudo* reference electrode. Experiments were run at scan rates of 100 mV s^{-1} in degassed THF solutions of the analyte (~1 mM) and supporting electrolyte (0.1 M [*n*Bu$_4$][PF$_6$]). Cyclic voltammograms were referenced against an internal standard (~1 mM ferrocene) and corrected for internal cell resistance using the BASi Epsilon software.

X-ray crystallography details

Single crystals suitable for X-ray diffraction were grown by slow evaporation of CH_2Cl_2 (**10**, **12**, **13**, **15**, $\mathbf{10}^{\bullet-}$) or $CHCl_3$ (**9**) solutions, or diffusion of hexanes into a concentrated THF solution ($\mathbf{10}^{\bullet\bullet 2-}$). To grow single crystals of $\mathbf{16}^{-}$, the cobaltocenium salt was first stirred for 30 min with

[*n*Bu$_4$N][Br] in CH_2Cl_2. The resulting solution was then filtered and concentrated *in vacuo*. Finally, crystals appeared upon diffusion of hexanes into a concentrated THF solution. Samples were mounted on a MiTeGen polyimide micromount with a small amount of Paratone N oil. X-ray measurements were made on a Bruker Kappa Axis Apex2 diffractometer (**9**, **12**, **13**, **15**, **10**$^{\bullet-}$, **10**$^{\bullet\bullet 2-}$ and **16**$^{-}$) or Nonius KappaCCD Apex2 diffractometer (**10**) at a temperature of 110 K. Initial indexing indicated that the sample crystal for **12** was non-merohedrally twinned. The twin law was determined to be:

−1.00038	−0.00037	−0.00061
0.00057	−0.99976	0.00063
0.92946	0.44676	1.00014

which represents a −179.9° rotation about [0 0 −1]. The twin fraction was included in the refinement as an adjustable parameter (*vide infra*).

The data collection strategy included a number of ω and φ scans which collected data over a range of angles, 2θ. The frame integration was performed using SAINT.[4] The resulting raw data were scaled and absorption corrected using a multi-scan averaging of symmetry equivalent data using SADABS (**9**, **10**, **13**, **15**, **10**$^{\bullet-}$, **10**$^{\bullet\bullet 2-}$, **16**$^{-}$),[5] or TWINABS (**12**).[6] The structures were solved by using a dual space methodology using the SHELXT program.[7] All non-hydrogen atoms were obtained from the initial solution. The hydrogen atoms were introduced at idealized positions and were allowed to refine isotropically (**9**, **10**, **12**, **13**, **15**), or allowed to ride on the parent atom (**10**$^{\bullet-}$, **10**$^{\bullet\bullet 2-}$), or treated in a mixed fashion (**16**$^{-}$). The twin fraction of **12** refined to a value of 0.07489. The structural model was fit to the data using full matrix least-squares based on F^2. The calculated structure factors included corrections for anomalous dispersion from the usual tabulation. The difference map of **10**$^{\bullet\bullet 2-}$ showed regions of electron density that could not be accurately modeled to something that makes chemical sense. Thus the PLATON SQUEEZE

program[8] was used, and analysis was continued on these data. The structure was refined using the SHELXL-2014 program from the SHELXT suite of crystallographic software.[9] See Table S3 and CCDC 1543994−1544001 for additional crystallographic data.

Table S2. Selected bond lengths and angles for solid-state structures of various products.

	9	**10**	**$10^{\bullet-}$**	**$10^{\bullet\bullet 2-}$**	**12**	**13**	**16^{-}**
N1-N2 (Å)	1.2896(16)	1.297(3)	1.353(3)	1.357(3)	1.2997(19)	1.288(2)	1.297(4)
N3-N4 (Å)	1.3206(16)	1.330(3)	1.366(3)	1.375(3)	1.280(2)	1.284(2)	1.287(4)
N5-N6 (Å)	−	1.299(3)	1.329(3)	1.371(3)	−	−	−
N7-N8 (Å)	−	1.332(3)	1.301(3)	1.359(3)	−	−	−
B1-N1 (Å)	1.5743(19)	1.572(4)	1.541(4)	1.540(3)	1.596(2)	1.573(3)	1.583(5)
B1-N5 (Å)	−	−	−	−	1.532(2)	1.516(3)	1.442(5)
C2-N5 (Å)	−	−	−	−	1.295(2)	1.304(3)	1.327(4)
N1-B1-N5 (°)	−	−	−	−	107.37(13)	104.45(17)	107.9(3)
B1-N5-C2 (°)	−	−	−	−	126.62(14)	120.36(18)	116.8(3)
N3-B2-O2 (°)	−	−	−	−	101.53(14)	101.62(17)	100.5(3)
B2-O3-C2 (°)	−	−	−	−	116.48(14)	118.97(17)	117.0(3)

Table S3. X-ray diffraction data collection and refinement details

	9	**10**	**12**	**13**	**15**	**10^{-}**	**10$^{\bullet-2-}$**	**16^{-}**
Chemical Formula	$C_{13}H_9BCl_2N_5O_2$	$C_{28}H_{16}B_2N_{10}O_4$	$C_{14}H_{10}B_2F_3N_5O_3$	$C_{15}H_{10}B_2Cl_2F_2N_5O_3$	$C_{16}H_{11}BN_5O_2$	$C_{39.50}H_{39}B_2Cl_3CoN_{10}O_4$	$C_{48}H_{36}B_2Co_2N_{10}O_4$	$C_{34}H_{49}B_2F_2N_6O_4$
FW (g/mol)	408.43	578.13	374.89	438.80	317.12	894.63	956.35	665.41
Crystal Habit	Red Prism	Red Plate	Red Plate	Purple Plate	Red Plate	Red Prism	Green Plate	Blue Prism
Crystal System	Monoclinic	Monoclinic	Triclinic	Triclinic	Triclinic	Triclinic	Monoclinic	orthorhombic
Space Group	$P2_1/n$	$P2_1/c$	$P\bar{1}$	$P\bar{1}$	$P\bar{1}$	$P\bar{1}$	$C2/c$	$Pna2_1$
T (K)	110	110	110	110	110	110	110	110
λ (Å)	0.71073	1.54178	0.71073	0.71073	0.71073	0.71073	0.71073	0.71073
a (Å)	9.998(5)	12.881(3)	7.200(3)	7.26(3)	10.470(4)	9.674(4)	38.958(14)	27.391(12)
b (Å)	10.986(6)	22.431(6)	7.899(3)	11.186(5)	11.193(4)	13.911(6)	9.286(3)	14.196(7)
c (Å)	16.990(10)	9.388(2)	15.294(8)	12.213(4)	13.763(4)	15.088(6)	26.485(10)	9.375(3)
α (deg)	90	90	91.890(12)	115.101(13)	91.150(9)	71.773(13)	90	90
β (deg)	104.739(14)	91.295(9)	100.25(2)	97.410(17)	91.444(8)	86.992(9)	96.663(13)	90
γ (deg)	90	90	112.364(10)	96.153(13)	115.938(8)	87.645(7)	90	90
V (Å^3)	1804.8(17)	2711.8(12)	786.7(6)	876.7(6)	1449.0(8)	1925.4(13)	9516(6)	3645(3)
Z	4	4	2	2	4	2	8	4
ρ (g/cm^3)	1.503	1.416	1.583	1.662	1.454	1.543	1.335	1.212
μ (cm^{-1})	0.528	0.820	0.135	0.421	0.100	0.712	0.751	0.086
R_1,[a] wR_2[b] [I > 2σ]	0.0465, 0.1013	0.0483, 0.1001	0.0483, 0.1001	0.0507, 0.1049	0.0382, 0.1009	0.0563, 0.1134	0.0385, 0.0760	0.0486, 0.1159
R_1, wR_2 (all data)	0.0759, 0.1157	0.0967, 0.1194	0.0590, 0.1462	0.0877, 0.1232	0.0491, 0.1083	0.1072, 0.1334	0.0685, 0.0828	0.0707, 0.1289
GOF[c]	1.032	1.025	1.120	1.028	1.045	1.031	0.904	1.043

[a] $R_1 = \Sigma(|F_o| - |F_c|) / \Sigma F_o$, [b] $wR_2 = [\Sigma(w(F_o^2 - F_c^2)^2) / \Sigma(w F_o^4)]^{½}$, [c] GOF = $[\Sigma(w(F_o^2 - F_c^2)^2) /$ (No. of reflns. - No. of params. $)]^{½}$

General Experimental for Complexes 9-13

Formazan **7** (0.33 g, 1.2 mmol) was dissolved in dry toluene (40 mL). NEt_3 (0.36 g, 0.49 mL, 3.5 mmol) was then added slowly and the solution stirred for 10 min before BF_3•OEt_2 (0.83 g, 0.72 mL, 5.8 mmol) was added and the solution was heated with stirring at 80 ºC for 18 h. The solution immediately turned dark blue/purple. After cooling to 22 ºC, the reaction mixture was poured into a separatory funnel containing deionized H_2O (100 mL). The purple toluene solution was then washed with deionized H_2O (3 × 100 mL), dried over $MgSO_4$, gravity filtered and concentrated *in vacuo*. The resulting residue contained a mixture of compounds **7** and **9**–**13**. These compounds were separated (**9**: R_f = 0.82; **10**: R_f = 0.76; **11**: R_f = 0.61; **7**: R_f = 0.39; **12**: R_f = 0.31; **13**: R_f = 0.22) by column chromatography (CH_2Cl_2, silica). Additional column chromatography (10:1 toluene:EtOAc, silica) was required to separate compounds **9** and **10**, and **12** and **13**. See Table S4 for compound distributions under a variety of experimental conditions.

Table S4. Varied reaction conditions and the resulting product distributions.

Equiv. NEt_3	Equiv. BF_3•OEt_2	Reaction Time (h)	Temp. (°C)	Conc. of 7 (mg mL^{-1})	Distribution of Products (%)					
					7	**9**	**10**	**11**	**12**	**13**
3	5	16	80	10	27	24	7	11	3	28
1	1	16	80	10	92	–	–	8	–	–
6	10	16	80	10	63	3	29	2	–	3
3	5	8	80	10	68	6	1	22	1	2
3	5	32	80	10	6	6	2	17	1	68
3	5	16	50	10	66	4	3	21	–	6
3	5	16	110	10	15	21	11	7	–	46
3	5	16	80	5	28	1	2	21	3	45
3	5	16	80	20	18	4	11	26	4	37

9

M.p. 244–246 °C. ^{1}H NMR (400.1 MHz, $CDCl_3$): δ 7.80 (d, $^{3}J_{HH}$ = 9 Hz, 2H, aryl C*H*), 7.39–7.34 (m, 4H, aryl C*H*), 7.13–7.11 (m, 2H, aryl C*H*), 7.05–7.00 (m, 4H, aryl C*H*), 6.94 (d, $^{3}J_{HH}$ = 8 Hz, 2H, aryl C*H*) 6.60–6.58 (m, 2H, aryl C*H*). ^{13}C{^{1}H} NMR (150.7 MHz, $CDCl_3$): δ 155.7, 148.0, 138.1, 135.9, 132.6, 131.9, 130.3, 129.2, 128.4, 125.0, 124.1, 122.7, 115.7, 114.6. ^{11}B NMR (128.3 MHz, $CDCl_3$): δ 1.0 (s). FT-IR (ATR): 2235 (m), 1590 (m), 1483 (m), 1382 (m), 1309 (s), 1252 (s), 1079 (s), 1046 (s), 988 (m), 960 (m) cm^{-1}. UV-vis (CH_2Cl_2): λ_{max} 535 nm (ε = 28,100 M^{-1} cm^{-1}), 440 nm (ε = 12,600 M^{-1} cm^{-1}), 296 nm (ε = 21,500 M^{-1} cm^{-1}). Mass Spec. (EI, +ve mode): exact mass calculated for $[C_{28}H_{16}B_2N_{10}O_4]^+$: 578.1542; exact mass found: 578.1531; difference: –1.9 ppm.

10

M.p. not observed (>250 °C). ^{1}H NMR (400.1 MHz, $CDCl_3$): δ 7.88−7.85. (m, 2H, aryl C*H*), 7.56–7.52 (m, 2H, aryl C*H*), 7.36–7.32 (m, 2H, aryl C*H*), 7.23 (d, $^{3}J_{HH}$ = 8 Hz, 2H, aryl C*H*), 7.17–7.12 (m, 6H, aryl C*H*), 6.84−6.81 (m, 2H, aryl C*H*). ^{13}C{^{1}H} NMR (150.7 MHz, $CDCl_3$): δ 156.6, 147.5, 136.4, 136.3, 132.6, 132.1, 131.0, 126.4, 125.1, 122.9, 122.3, 117.1, 116.4, 112.9. ^{11}B NMR (128.3 MHz, $CDCl_3$): δ 1.1 (s). FT-IR (ATR): 2923 (m), 2853 (w), 2243 (m), 1592 (m), 1481 (m), 1323 (s), 1247 (s), 1148 (m), 1084 (s), 995 (m), 971 (m) cm^{-1}. UV-vis (CH_2Cl_2): λ_{max} 605 nm (ε = 19,400 M^{-1} cm^{-1}), 569 nm (ε = 20,500 M^{-1} cm^{-1}), 415 nm (8,800 M^{-1} cm^{-1}), 319 nm (19,700 M^{-1} cm^{-1}). Mass Spec. (EI, +ve mode): exact mass calculated for $[C_{28}H_{16}B_2N_{10}O_4]^+$: 578.1542; exact mass found: 578.1547; difference: +0.9 ppm.

11

M.p. 165–166 ºC. ^{1}H NMR (400.1 MHz, $CDCl_3$): δ 9.56 (s, 1H, OH), 8.14 (d, $^{3}J_{HH}$ = 9 Hz, 1H, aryl C*H*), 7.82 (d, $^{3}J_{HH}$ = 9 Hz, 1H, aryl C*H*), 7.53 (m, 1H, aryl C*H*), 7.35–7.34 (m, 1H, aryl C*H*), 7.20–7.16 (m, 2H, aryl C*H*), 7.08–7.06 (m, 2H, aryl C*H*). ^{13}C{^{1}H} NMR (150.7 MHz, $CDCl_3$): δ 157.6, 153.4, 135.9, 135.8, 133.1, 133.0, 125.3, 123.3, 121.5, 120.3, 117.0, 115.6, 115.3, 113.3. ^{11}B NMR (128.3 MHz, $CDCl_3$): δ 0.0 (d, $^{1}J_{BF}$ = 37 Hz). ^{19}F NMR (376.1 MHz, $CDCl_3$): δ –151.1 (q, $^{1}J_{FB}$ = 37 Hz). FT-IR (ATR): 3351 (br, m), 2924 (m), 2853 (w), 2244 (m), 1594 (s), 1378 (s), 1310 (s), 1148 (m), 1102 (m), 995 (s) cm^{-1}. UV-vis (CH_2Cl_2): λ_{max} 619 nm (ε = 11,700 M^{-1} cm^{-1}), 577 nm (ε = 13,500 M^{-1} cm^{-1}), 445 nm (ε = 5,800 M^{-1} cm^{-1}), 318 nm (ε = 11,300 M^{-1} cm^{-1}). Mass Spec. (EI, +ve mode): exact mass calculated for $[C_{14}H_9BFN_5O_2]^{+}$: 309.0833; exact mass found: 309.0843; difference: +3.2 ppm.

12

M.p. 217–219 ºC. ^{1}H NMR (400.1 MHz, $CDCl_3$): δ 10.50 (s, 1H, OH), 8.05–8.04 (m, 1H, aryl C*H*), 7.71–7.70 (m, 1H, aryl C*H*), 7.51–7.48 (m, 1H, aryl C*H*), 7.45 (br s, 1H, NH), 7.35–7.33 (m, 1H, aryl C*H*), 7.15–7.10 (m, 3H, aryl C*H*), 7.02–6.99 (m, 1H, aryl C*H*). ^{13}C{^{1}H} NMR (150.7 MHz, $CDCl_3$): δ 159.3, 152.7, 152.4, 136.0, 134.5, 132.3, 129.6, 124.6, 122.7, 120.9, 120.1, 116.1, 115.9. ^{11}B NMR (128.3 MHz, $CDCl_3$): δ 1.6 (d, $^{1}J_{BF}$ = 30 Hz), 0.4 (t, $^{1}J_{BF}$ = 28 Hz). ^{19}F NMR (376.1 MHz, $CDCl_3$): δ (–125.0)–(–124.7) (m), –149.8 (q, $^{1}J_{FB}$ = 28 Hz). FT-IR (ATR): 3314 (m), 3302 (m), 2924 (m), 2854 (w), 1646 (m), 1600 (m), 1458 (m), 1406 (s), 1306 (s), 1099 (m), 1116 (m), 1002 (s), 905 (m) cm^{-1}. UV-vis (CH_2Cl_2): λ_{max} 560 nm (ε = 27,600 M^{-1} cm^{-1}), 412 nm (ε = 7,600 M^{-1} cm^{-1}), 348 nm (ε = 4,100 M^{-1} cm^{-1}), 260 nm (ε = 4,600 M^{-1} cm^{-1}).

Mass Spec. (EI, +ve mode): exact mass calculated for $[C_{14}H_{10}B_2F_3N_5O_3]^+$: 374.0844; exact mass found: 374.0833; difference: −2.9 ppm.

13

M.p. 207–209 °C. ^{1}H NMR (400.1 MHz, $CDCl_3$): δ 7.82–7.76 (m, 2H, aryl C*H*), 7.69 (s, 1H, N*H*), 7.48–7.44 (m, 2H, aryl C*H*), 7.16–7.09 (m, 4H, aryl C*H*). ^{13}C{^{1}H} NMR (150.7 MHz, $CDCl_3$): δ 134.9, 134.1, 122.3, 122.1, 115.9, 115.8, 115.6, 115.5. ^{11}B NMR (128.3 MHz, $CDCl_3$): δ 1.6 (d, $^1J_{BF}$ = 33 Hz), 0.9 (d, $^1J_{BF}$ = 42 Hz). ^{19}F NMR (376.1 MHz, $CDCl_3$): δ –137.6 (q, $^1J_{FB}$ = 42 Hz), –149.8 (q, $^1J_{FB}$ = 33 Hz). FT-IR (ATR): 3169 (m), 1594 (m), 1431 (m), 1317 (s), 1286 (s), 1065 (s), 998 (m), 902 (m) cm^{-1}. UV-vis (CH_2Cl_2): λ_{max} 577 nm (ε = 35,900 M^{-1} cm^{-1}), 407 nm (ε = 6,800 M^{-1} cm^{-1}), 269 nm (14,600 M^{-1} cm^{-1}). Mass Spec. (EI, +ve mode): exact mass calculated for $[C_{14}H_9B_2F_2N_5O_3]^+$: 355.0860; exact mass found: 355.0861; difference: +0.3 ppm.

14

In air, cyanoacetic acid (0.21 g, 2.4 mmol) was dissolved in deionized H_2O (50 mL) containing NaOH (0.96 g, 24 mmol). This colourless solution was stirred for 45 min in an ice bath. Meanwhile, 2-aminobenzyl alcohol (0.59 g, 4.8 mmol) was mixed with concentrated HCl (1.2 mL) in deionized H_2O (15 mL). This solution was cooled in an ice bath for 10 min before a solution of sodium nitrite (0.38 g, 5.5 mmol) in deionized H_2O (10 mL) was cooled in an ice bath, and then added slowly to the 2-aminobenzyl alcohol solution over a 10 min period. This mixture was stirred in an ice bath for 30 min and then added slowly to the basic cyanoacetic acid solution. A dark red/orange colour persisted almost immediately, and a dark red/orange precipitate formed after a few min. The mixture was stirred in an ice bath for an additional 16 h

before ethyl acetate (250 mL) was added and the organic layer was isolated, washed with deionized H_2O (3 × 100 mL), dried over $MgSO_4$, gravity filtered and concentrated *in vacuo*. The resulting residue was purified by flash chromatography (CH_2Cl_2, neutral alumina) to afford formazan **14** as a dark red solid. Yield = 0.66 g, 87%. M.p. 185–187 ºC. ^{1}H NMR (400.1 MHz, DMSO-d_6): δ major isomer: 12.88 (s, 1H, NH), 7.66 (d, $^3J_{HH}$ = 9 Hz, 2H, aryl C*H*), 7.52 (d, $^3J_{HH}$ = 9 Hz, 2H, aryl C*H*), 7.40–7.35 (m, 4H, aryl C*H*), 5.81 (s, 2H, OH), 4.94 (s, 4H, CH_2). δ minor isomer: 11.72 (s, 1H, NH), 7.73−7.63 (m, 2H, aryl C*H*), 7.57−7.54 (m, 2H, aryl C*H*), 7.31−7.30 (m, 2H, aryl C*H*), 7.14−7.12 (m, 2H, aryl C*H*), 6.33 (s, 2H, OH), 5.02 (s, 2H, CH_2), 4.84 (s, 2H, CH_2). ^{13}C{^{1}H} NMR (150.7 MHz, DMSO-d_6), both isomers: δ 147.7, 144.3, 141.5, 140.6, 135.6, 130.9, 128.6, 128.2, 127.2, 124.4, 115.1, 112.6, 108.2, 62.7, 60.5, 58.3. FT-IR (ATR): 3535 (w), 3399 (m), 3215 (m), 2218 (m), 1587 (w), 1522 (m), 1461 (m), 1399 (m), 1265 (m), 1206 (m), 1014 (s), 758 (s), 722 (s) cm^{-1}. UV-vis (CH_2Cl_2): λ_{max} 438 nm (ε = 20,900 M^{-1} cm^{-1}), 294 nm (ε = 11,400 M^{-1} cm^{-1}), 267 nm (11,100 M^{-1} cm^{-1}). Mass Spec. (EI, +ve mode): exact mass calculated for $[C_{16}H_{15}N_5O_2]^+$: 309.1226; exact mass found: 309.1230; difference: +1.3 ppm.

15

Formazan **14** (0.66 g, 2.1 mmol) was dissolved in dry toluene (70 mL). NEt_3 (0.65 g, 0.90 mL, 6.4 mmol) was then added slowly and the solution was stirred for 10 min before BF_3•OEt_2 (1.49 g, 1.30 mL, 10.5 mmol) was added and the solution was heated with stirring at 80 ºC for 18 h. The solution gradually turned from dark red to dark purple during this time. After cooling to 22 ºC, deionized H_2O (10 mL) was added to quench any excess reactive boron-containing compounds. The purple toluene solution was then washed with deionized H_2O (3 × 50 mL), dried over $MgSO_4$, gravity filtered and concentrated *in vacuo*. The resulting residue was purified by flash chromatography (CH_2Cl_2, neutral alumina) to afford bis-methylene-hydroxy-substituted

complex **15** as a dark purple microcrystalline solid. Yield = 0.61 g, 92%. M.p. 235–237 °C. ^{1}H NMR (400.1 MHz, $CDCl_3$): δ 7.78–7.76 (m, 2H, aryl C*H*), 7.41–7.35 (m, 4H, aryl C*H*), 7.09–7.08 (m, 2H, aryl C*H*), 5.30–5.28 (m, 2H, CH_2) 5.15–5.12 (m, 2H, CH_2). ^{13}C{^{1}H} NMR (150.7 MHz, $CDCl_3$): δ 140.3, 134.3, 130.9, 128.2, 125.9, 125.7, 119.4, 114.9, 65.0. ^{11}B NMR (128.3 MHz, $CDCl_3$): δ –0.1 (s). FT-IR (ATR): 2986 (m), 2854 (m), 2235 (m), 1342 (s), 1299 (m), 1084 (s), 1008 (m), 988 (m), 761 (s), 707 (s) cm^{-1}. UV-vis (CH_2Cl_2): λ_{max} 596 nm (ε = 17,400 M^{-1} cm^{-1}), 558 nm (ε = 18,800 M^{-1} cm^{-1}), 395 nm (ε = 5,600 M^{-1} cm^{-1}), 292 nm (ε = 12,300 M^{-1} cm^{-1}). Mass Spec. (EI, +ve mode): exact mass calculated for $[C_{16}H_{12}BN_5O_2]^+$: 317.1084; exact mass found: 317.1082; difference: –0.6 ppm.

10$^{\bullet-}$

In a nitrogen-filled glovebox, **10** (0.034 g, 0.059 mmol) was dissolved in dry and degassed CH_2Cl_2 (5 mL). In a separate flask, cobaltocene (0.011 g, 0.059 mmol) was dissolved in dry and degassed CH_2Cl_2 (2 mL). The cobaltocene solution was added dropwise to a stirred solution of **10**. This mixture was stirred for an additional 30 min before it was filtered and the filtrate was collected. The solvent was removed *in vacuo* to yield a brown microcrystalline powder. Yield = 0.031 g, 68%. M.p. 226–228 °C. FT-IR (ATR): 3367 (m), 3109 (m), 2235 (m), 1667 (s), 1468 (m), 1415 (m), 1321 (s), 1232 (m), 1147 (m), 751 (m) cm^{-1}. UV-vis (CH_3CN): λ_{max} 520 nm (ε = 13,000 M^{-1} cm^{-1}), 477 nm (ε = 15,500 M^{-1} cm^{-1}), 262 nm (ε = 35,700 M^{-1} cm^{-1}). Mass Spec. (EI, −ve mode): exact mass calculated for $[C_{28}H_{16}B_2N_{10}O_4]^{\bullet-}$: 578.1542; exact mass found: 578.1538; difference: −0.7 ppm. Anal. Calcd. (%) for $C_{22}H_{19}N_5O$: C, 59.49; H, 3.42; N, 18.26. Found: C, 57.66; H, 3.31; N, 18.25.

$10^{\bullet\bullet 2-}$

In a nitrogen-filled glovebox, **10** (0.025 g, 0.043 mmol) was dissolved in dry CH_2Cl_2 (5 mL). In a separate flask, cobaltocene (0.016 g, 0.086 mmol) was dissolved in dry CH_2Cl_2 (3 mL). The cobaltocene solution was added dropwise to a stirred solution of **10**. This mixture was stirred for an additional 30 min before it was filtered and the precipitate was collected. The precipitate was collected by dissolving in CH_3CN before the solvent was removed *in vacuo* to yield a green microcrystalline powder. Yield = 0.034 g, 82%. M.p. not observed (>250 °C). FT-IR (ATR): 3359 (m), 3098 (m), 2234 (m), 1661 (s), 1467 (m), 1393 (m), 1321 (m), 1146 (m), 749 (m) cm^{-1}. UV-vis (CH_3CN): λ_{max} 694 nm (ε = 6,500 M^{-1} cm^{-1}), 477 nm (ε = 39,200 M^{-1} cm^{-1}), 330 nm (ε = 38,000 M^{-1} cm^{-1}), 261 nm (ε = 229,400 M^{-1} cm^{-1}). Mass Spec. (EI, −ve mode): exact mass calculated for $[C_{28}H_{16}B_2N_{10}O_4]^{2-}$: 289.0777; exact mass found: 289.0778; difference: +0.3 ppm. Anal. Calcd. (%) for $C_{48}H_{36}B_2Co_2N_{10}O_4 \bullet CH_2Cl_2$: C, 56.52; H, 3.68; N, 13.45. Found: C, 55.64; H, 3.60; N, 13.50.

16^-

In a nitrogen-filled glovebox, complex **13** (0.052 g, 0.15 mmol) was dissolved in dry CH_2Cl_2 (10 mL). In a separate flask, cobaltocene (0.28 g, 0.15 mmol) was dissolved in dry CH_2Cl_2 (5 mL). The cobaltocene solution was then added dropwise to a stirred solution of **13**. The resulting reaction mixture was stirred for an additional 30 min before it was filtered and concentrated *in vacuo*. The dark purple/blue residue obtained was dissolved in toluene (10 mL), before pentane (10 mL) was added to this solution, and the mixture was left in the freezer overnight (−35 °C). After this time, a dark purple microcrystalline powder had formed, which was collected by filtration as cobaltocenium salt **16^-**. Yield = 0.051 g, 58%. M.p. 116–118 °C. ^{1}H NMR (400.1

MHz, CD_2Cl_2): δ 7.70 (d, $^3J_{HH}$ = 8 Hz, 1H, aryl C*H*), 7.64 (d, $^3J_{HH}$ = 8 Hz, 1H, aryl C*H*), 7.31–7.26 (m, 2H, aryl C*H*), 7.02–6.96 (m, 4H, aryl C*H*), 5.75 (s, 10H, $CoCp_2^+$ C*H*). $^{13}C\{^1H\}$ NMR (150.7 MHz, CD_2Cl_2): δ 157.8, 157.5, 145.9, 145.8, 134.4, 133.9, 131.2, 130.9, 120.7, 120.0, 114.7, 114.3, 114.3, 114.0, 85.2. ^{11}B NMR (128.3 MHz, $CDCl_3$): δ 4.5 (br s), 3.1 (d, $^1J_{BF}$ = 40 Hz). ^{19}F NMR (376.1 MHz, $CDCl_3$): δ –136.4 (q, $^1J_{FB}$ = 28 Hz), –147.4 (q, $^1J_{FB}$ = 40 Hz). FT-IR (ATR): 3101 (m), 2961 (m), 2874 (w), 1601 (m), 1414 (m), 1315 (s), 1258 (m), 1147 (m), 1005 (m), 889 (m), 750 (s) cm^{-1}. UV-vis (CH_2Cl_2): λ_{max} 589 nm (ε = 18,000 M^{-1} cm^{-1}), 560 nm (ε = 17,000 M^{-1} cm^{-1}), 275 nm (ε = 2,500 M^{-1} cm^{-1}), 263 nm (ε = 20,700 M^{-1} cm^{-1}). Mass Spec. (EI, −ve mode): exact mass calculated for $[C_{14}H_8B_2F_2N_5O_3]^-$ 354.0781; exact mass found: 354.0796; difference: +4.2 ppm.

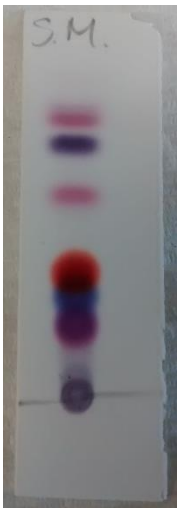

Figure S1. Silica TLC plate showing the separation of 6 components of the reaction mixture of formazan **7** with BF_3•OEt_2 and NEt_3.

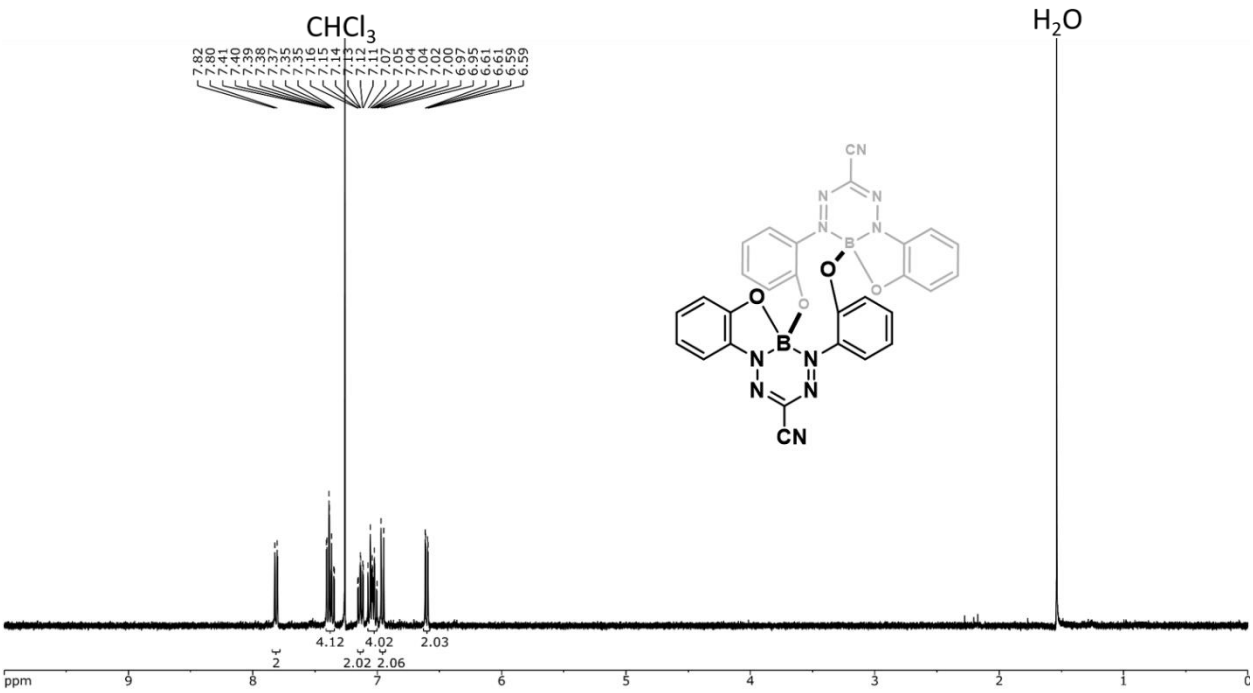

Figure S2. ^{1}H NMR spectrum of **9** in $CDCl_3$.

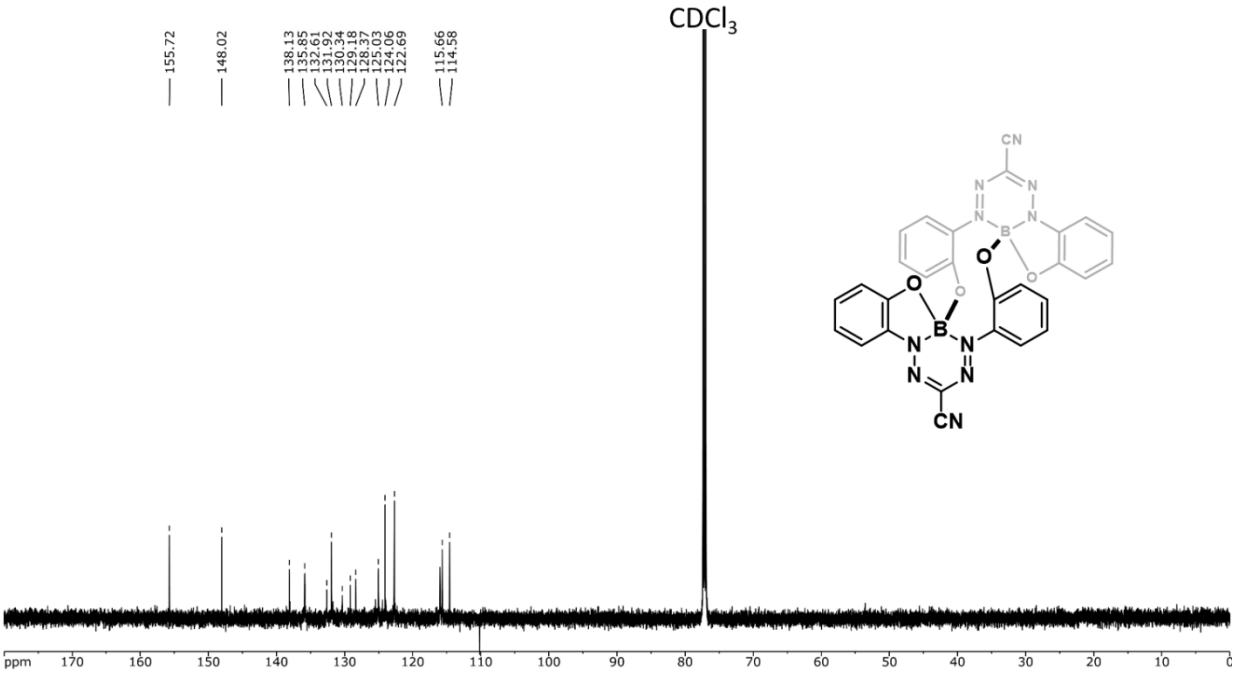

Figure S3. $^{13}C\{^{1}H\}$ NMR spectrum of **9** in $CDCl_3$.

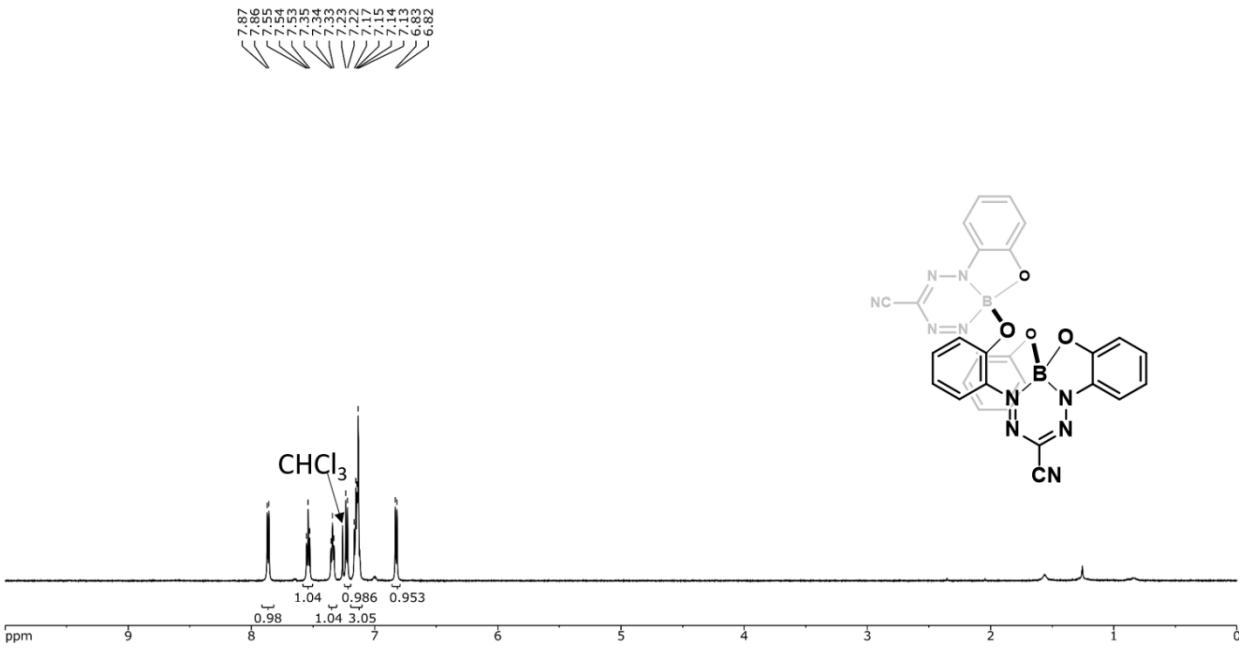

Figure S4. ^{1}H NMR spectrum of **10** in $CDCl_3$.

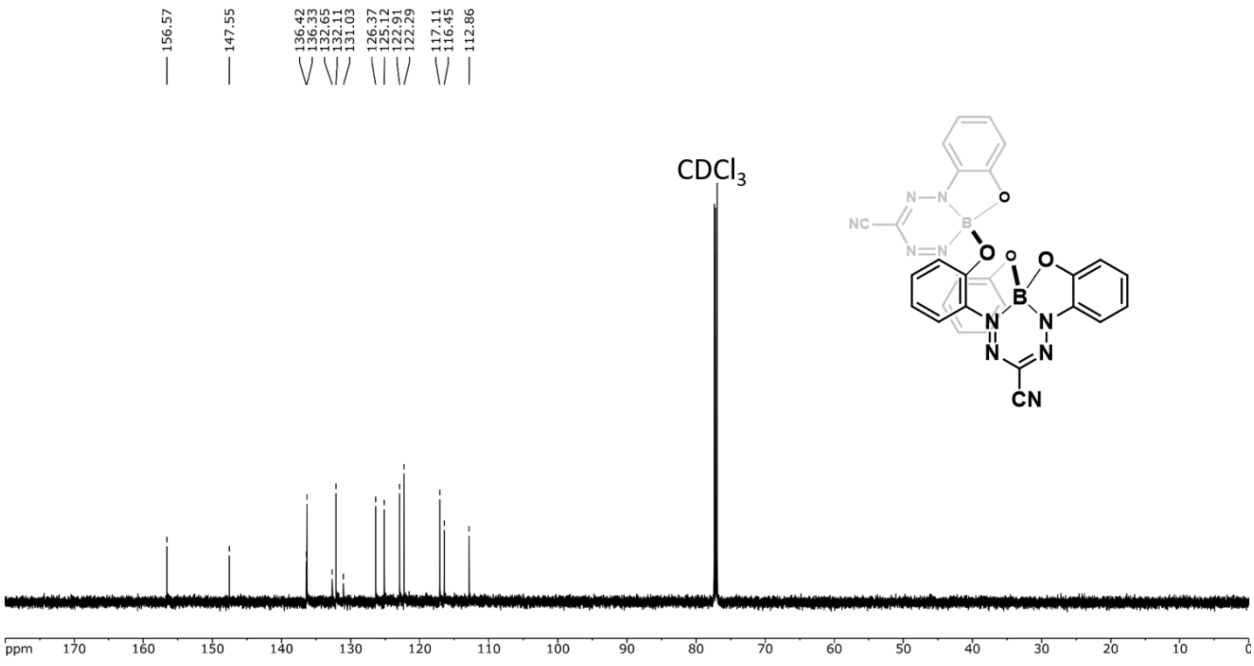

Figure S5. $^{13}C\{^{1}H\}$ NMR spectrum of **10** in $CDCl_3$.

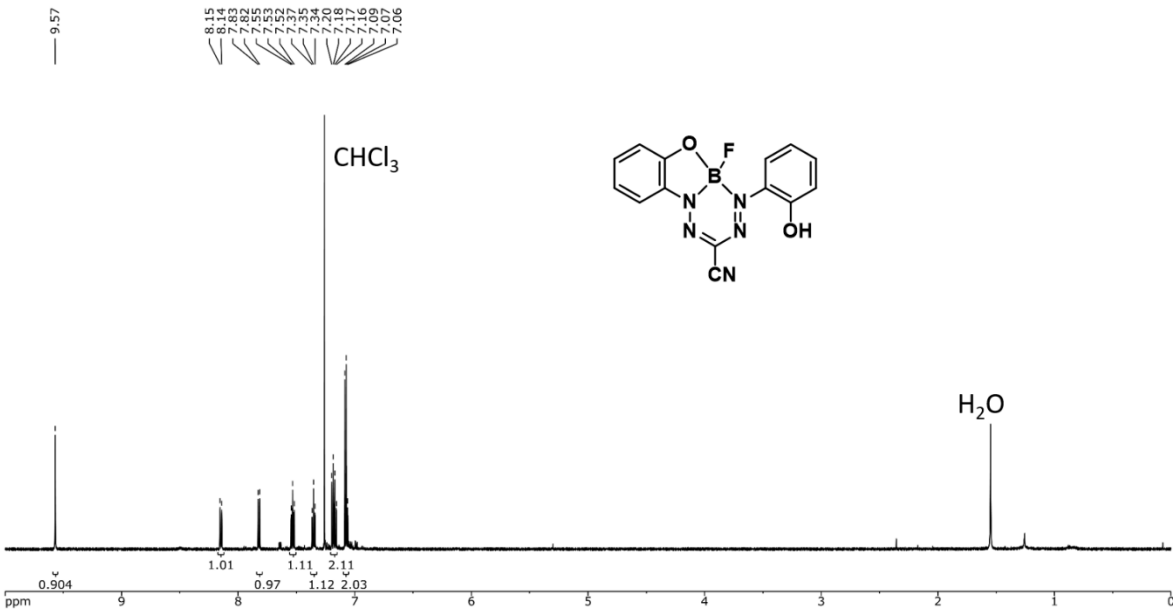

Figure S6. ^{1}H NMR spectrum of **11** in $CDCl_3$.

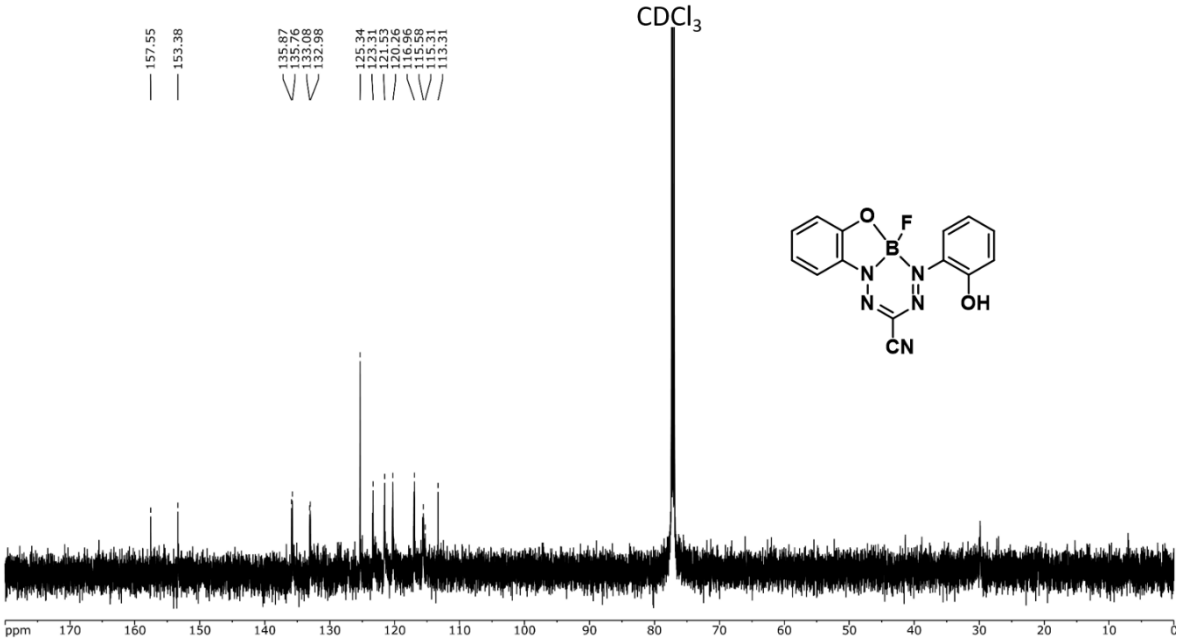

Figure S7. $^{13}C\{^{1}H\}$ NMR spectrum of **11** in $CDCl_3$. This spectrum was rapidly collected for a saturated solution of compound **11**. Efforts to improve the S/N ratio were thwarted by the conversion of **11** to formazan **7** in solution.

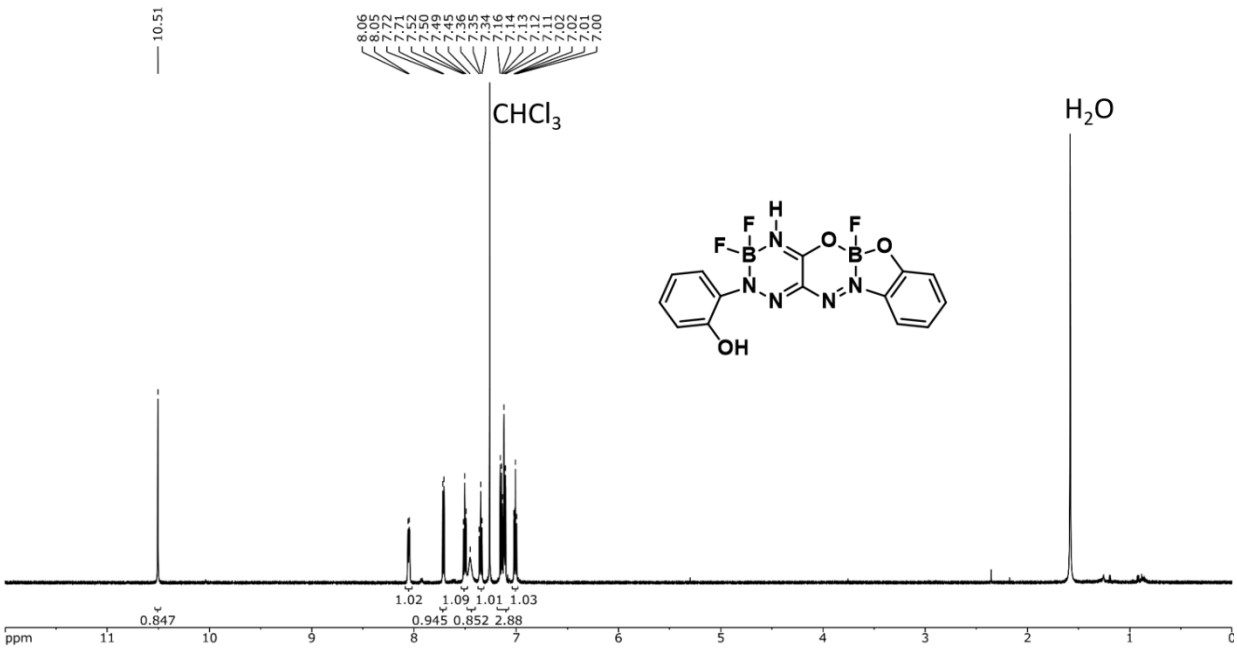

Figure S8. ^{1}H NMR spectrum of **12** in $CDCl_3$.

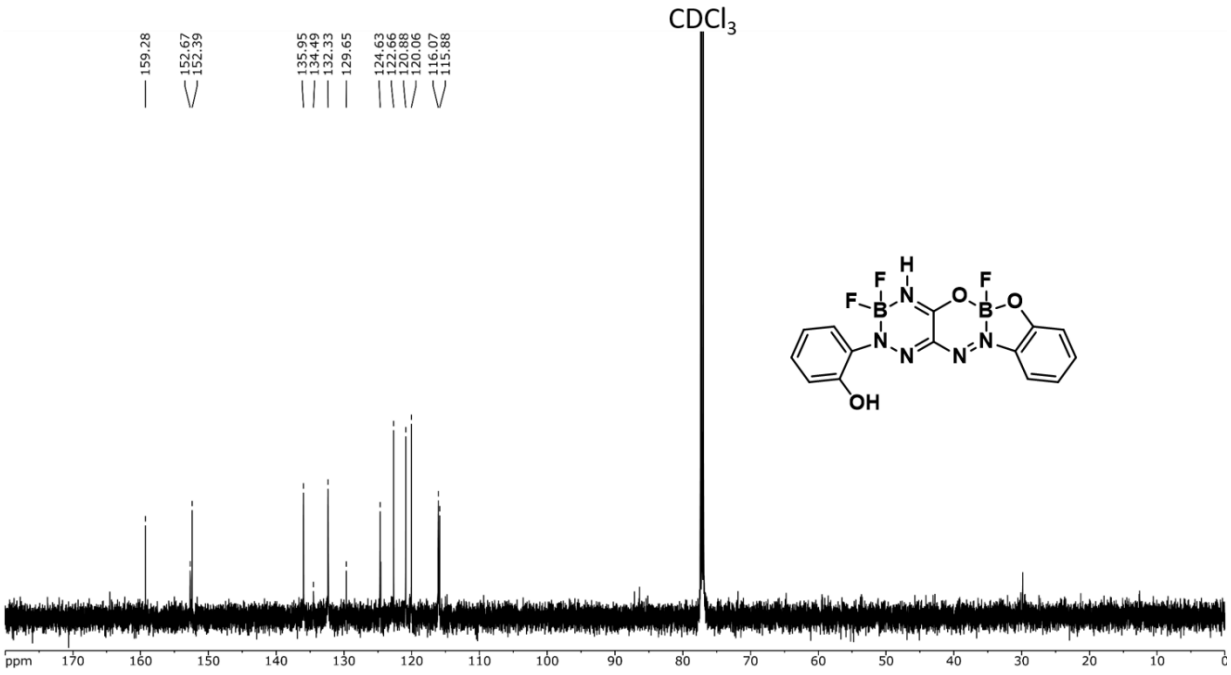

Figure S9. $^{13}C\{^{1}H\}$ NMR spectrum of **12** in $CDCl_3$.

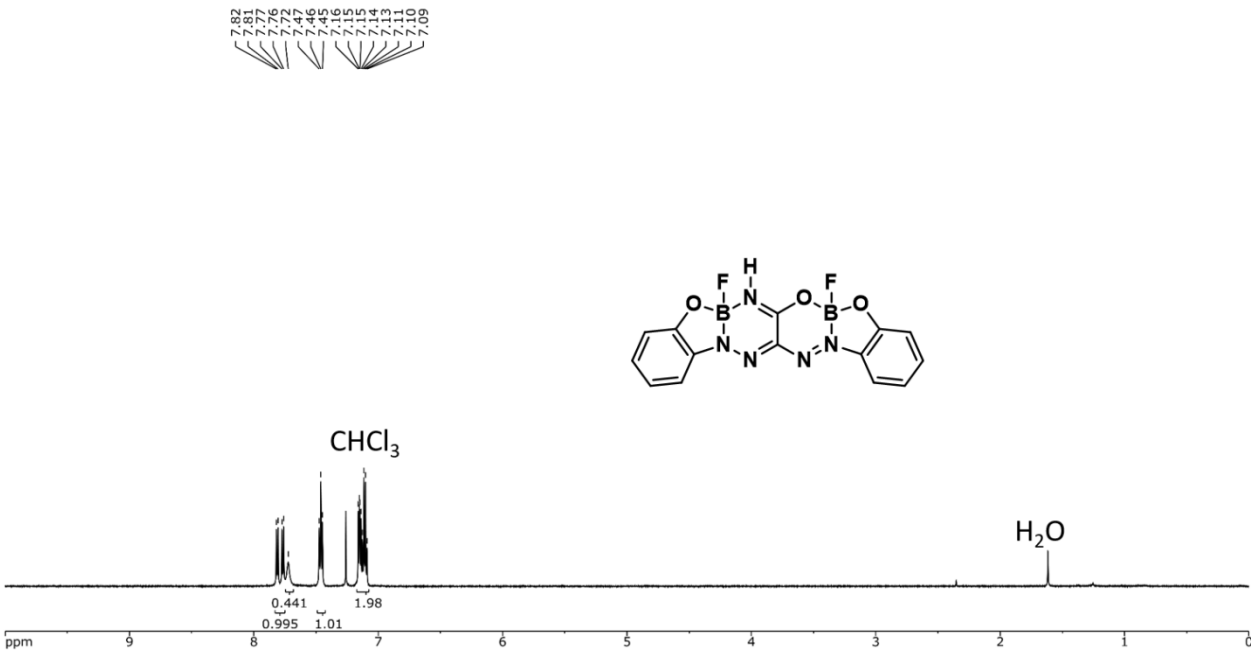

Figure S10. ^{1}H NMR spectrum of **13** in $CDCl_3$.

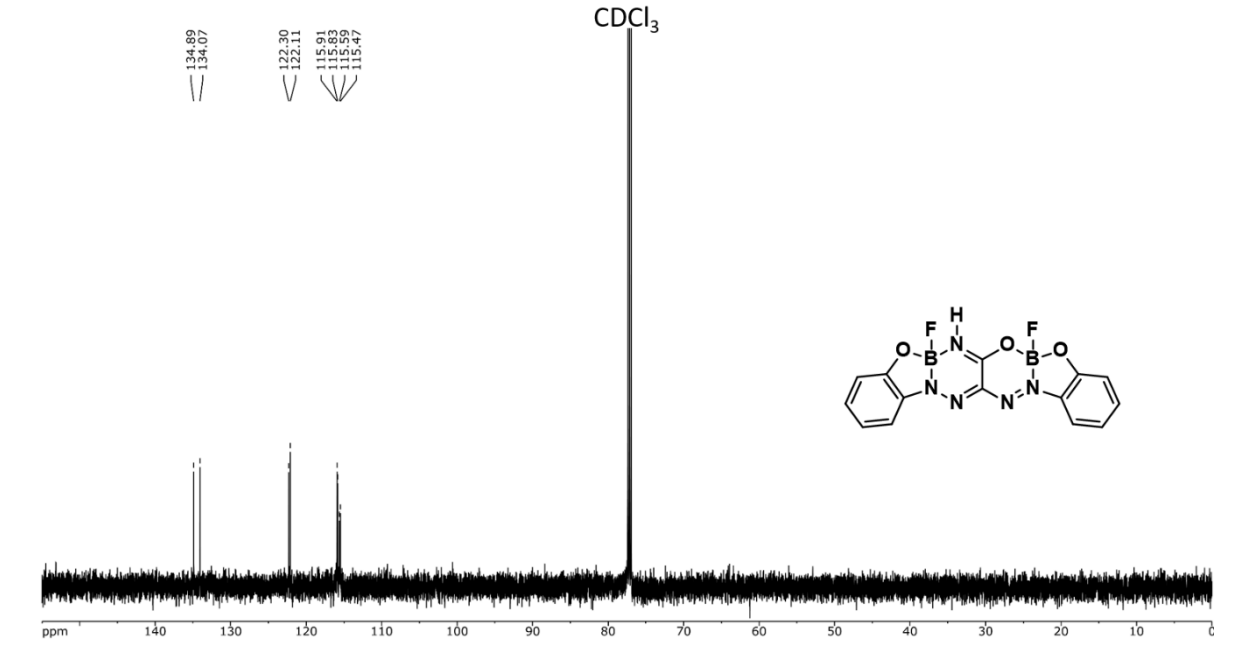

Figure S11. $^{13}C\{^{1}H\}$ NMR spectrum of **13** in $CDCl_3$.

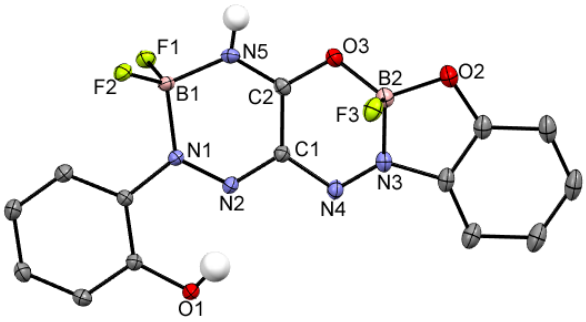

Figure S12. Solid-state structure of **12**. Thermal displacement ellipsoids are shown at the 50% probability level and hydrogen atoms, aside from those on N5 and O1, have been removed for clarity.

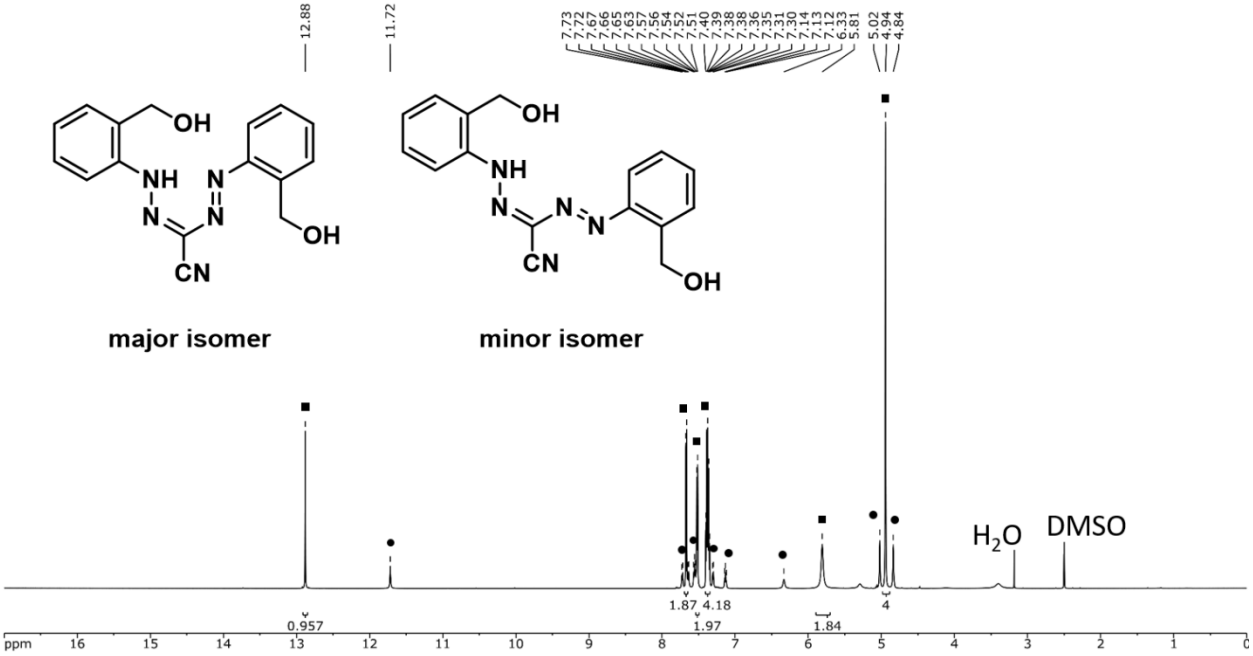

Figure S13. ^{1}H NMR spectrum of **14** in DMSO-d_6. Signals due to the major isomer have been marked with black squares, and those due to the minor isomer have been marked with black circles. Only signals from the major isomer have been integrated.

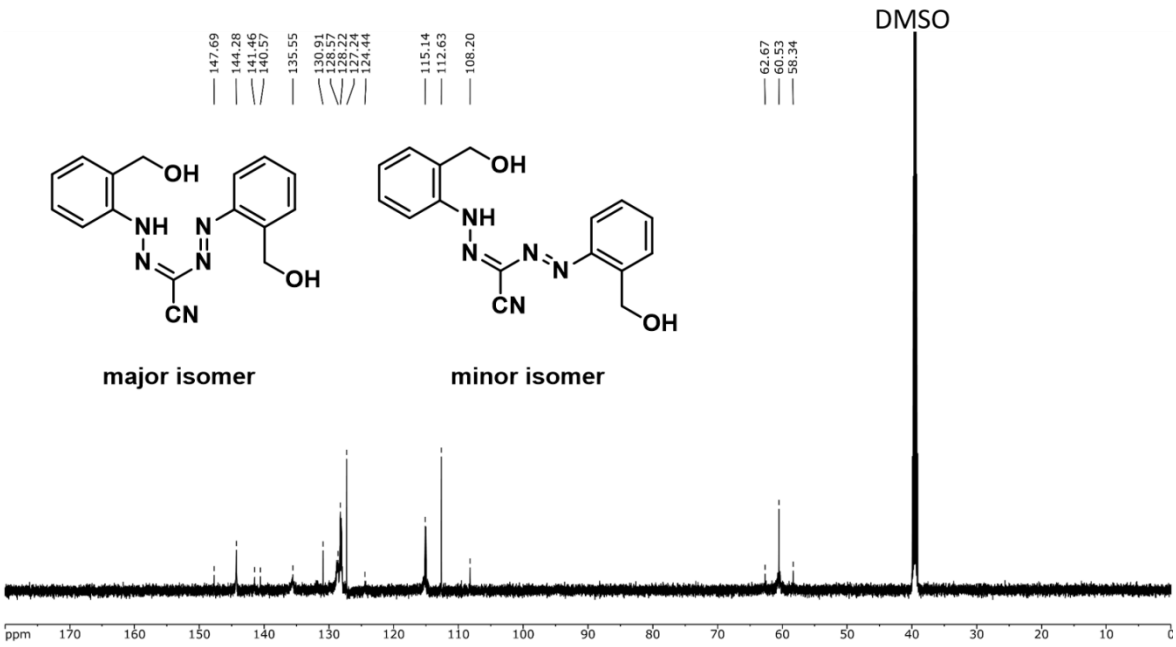

Figure S14. $^{13}C\{^{1}H\}$ NMR spectrum of **14** in DMSO-d_6. Formazan **14** was sparingly soluble in common NMR solvents. This spectrum was collected for a saturated solution over 10,000 scans on a 600 MHz NMR spectrometer.

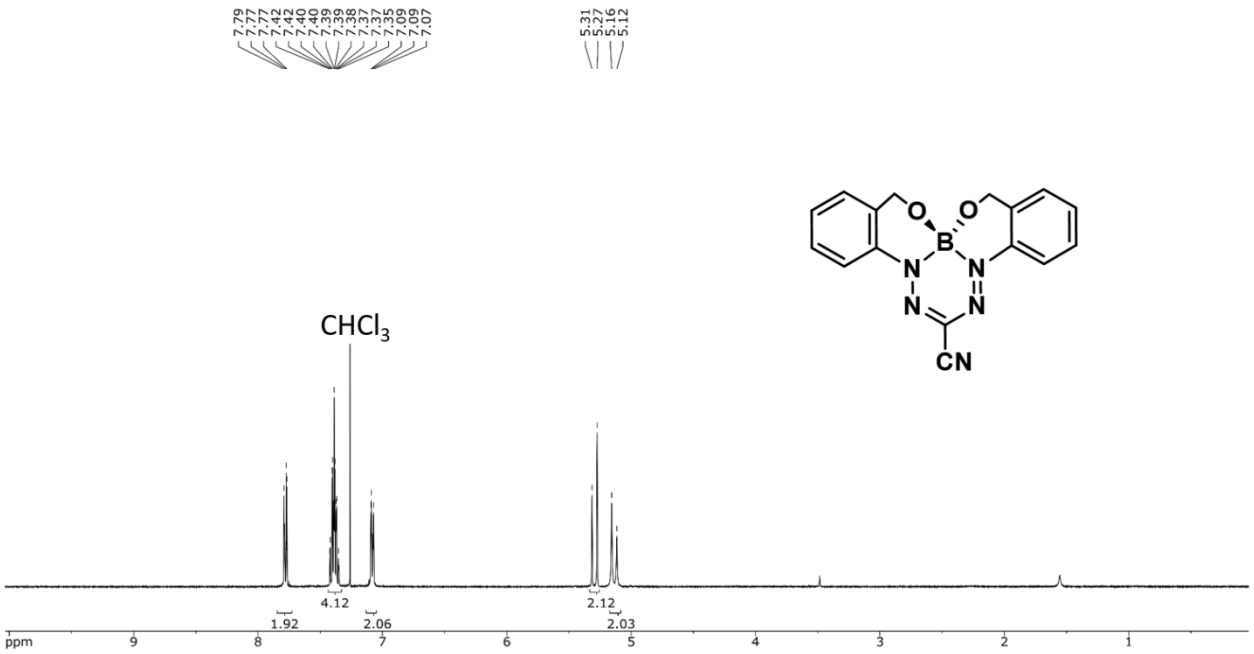

Figure S15. ^{1}H NMR spectrum of **15** in $CDCl_3$.

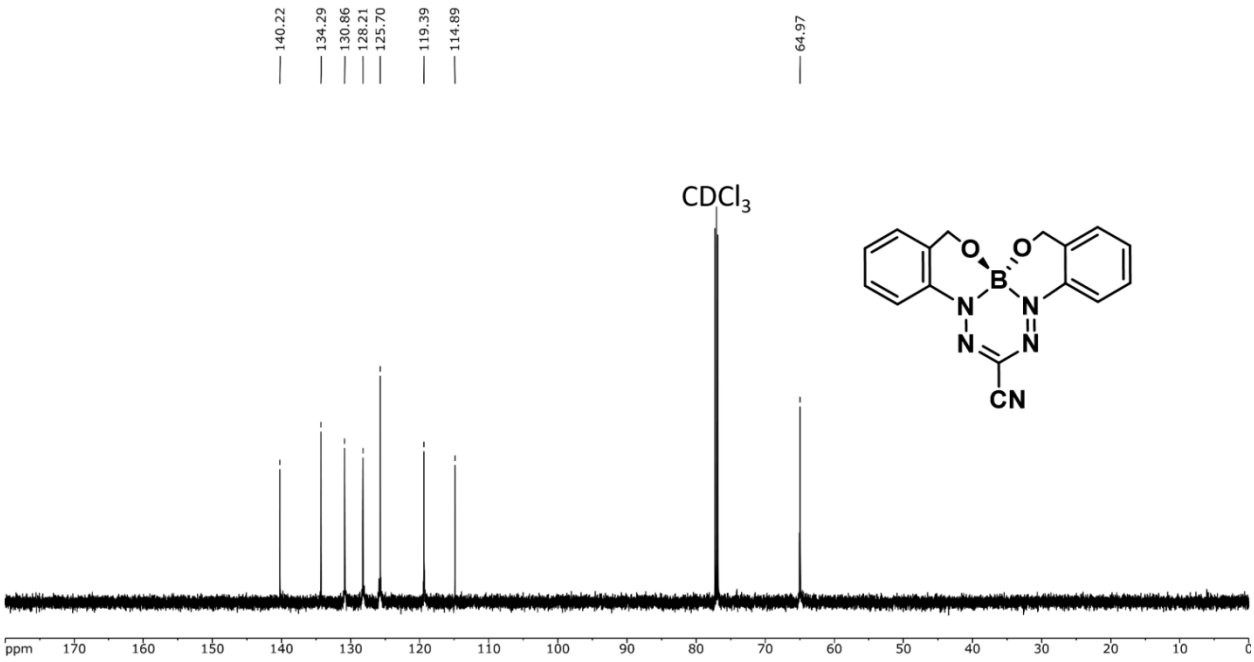

Figure S16. $^{13}C\{^{1}H\}$ NMR spectrum of **15** in $CDCl_3$.

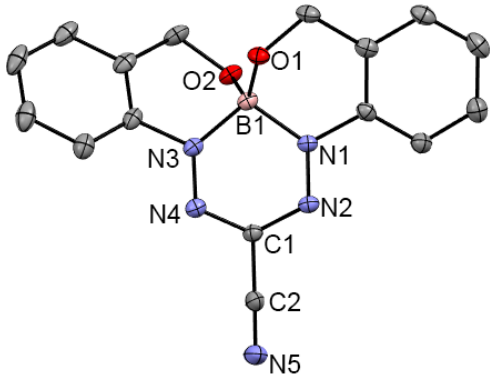

Figure S17. Solid-state structure of **15**. Thermal displacement ellipsoids are shown at the 50% probability level and hydrogen atoms have been removed for clarity.

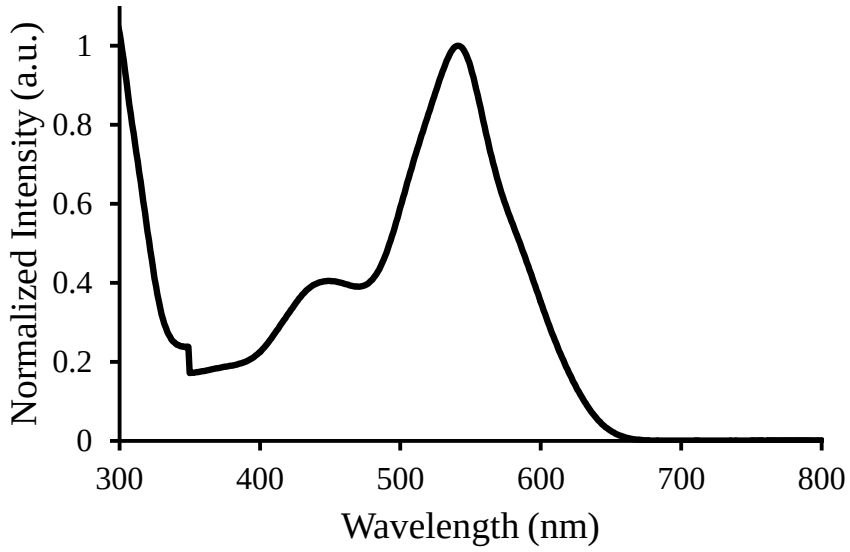

Figure S18. UV-vis absorption spectrum of complex **9** in toluene.

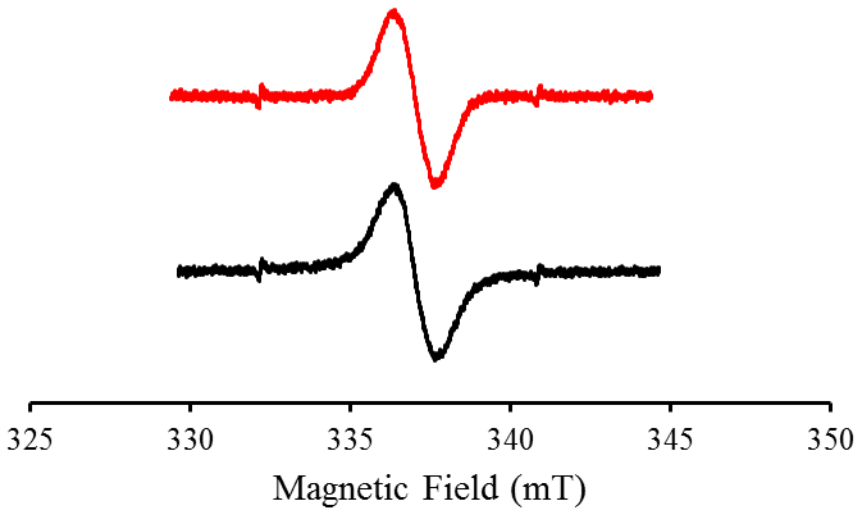

Figure S19. EPR spectra of $\mathbf{10}^{\bullet-}$ (red) and $\mathbf{10}^{\bullet\bullet 2-}$ (black) in CH_2Cl_2.

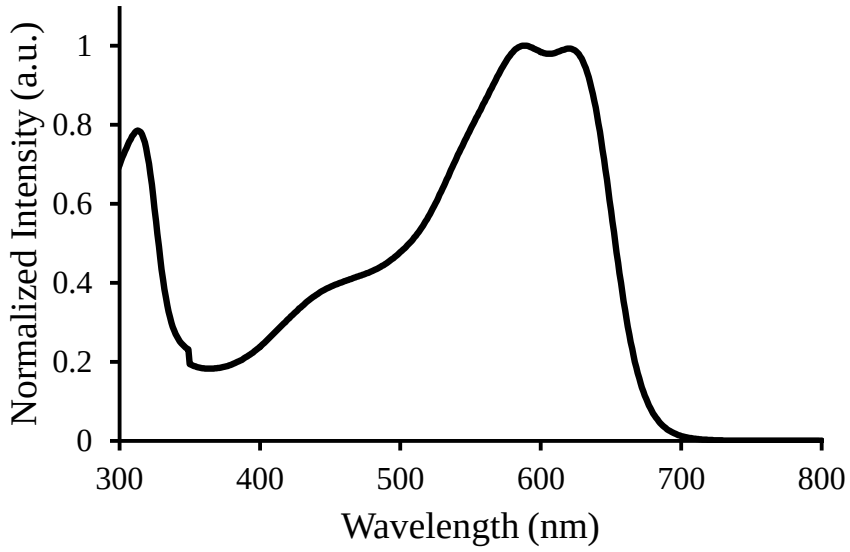

Figure S20. UV-vis absorption spectrum of complex **11** in toluene.

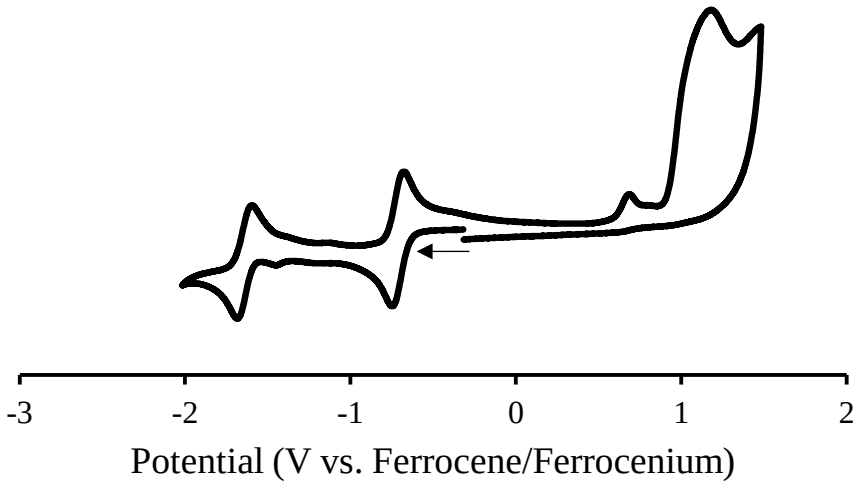

Figure S21. Cyclic voltammograms of complex **11** recorded at 100 mV s^{-1} in 1 mM CH_2Cl_2 solution containing 0.1 M [*n*Bu_4N][PF_6] as supporting electrolyte.

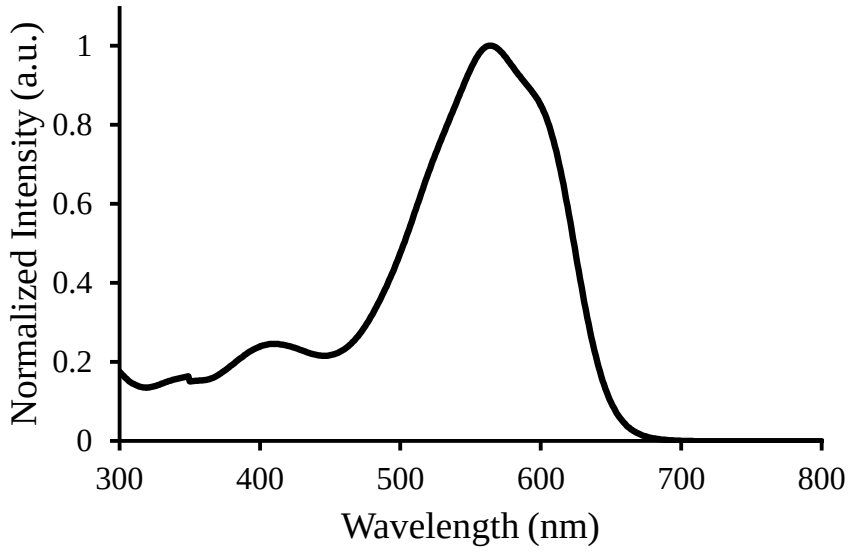

Figure S22. UV-vis absorption spectrum of complex **12** in toluene.

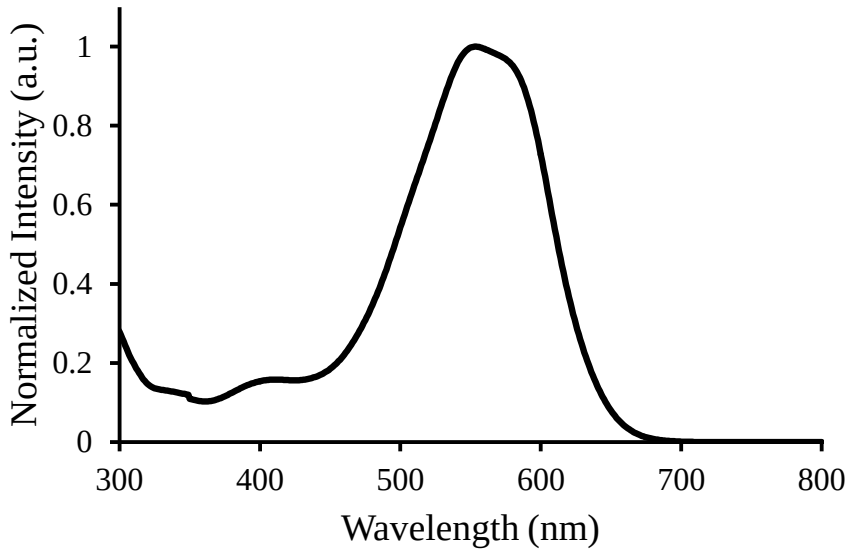

Figure S23. UV-vis absorption spectrum of complex **13** in toluene.

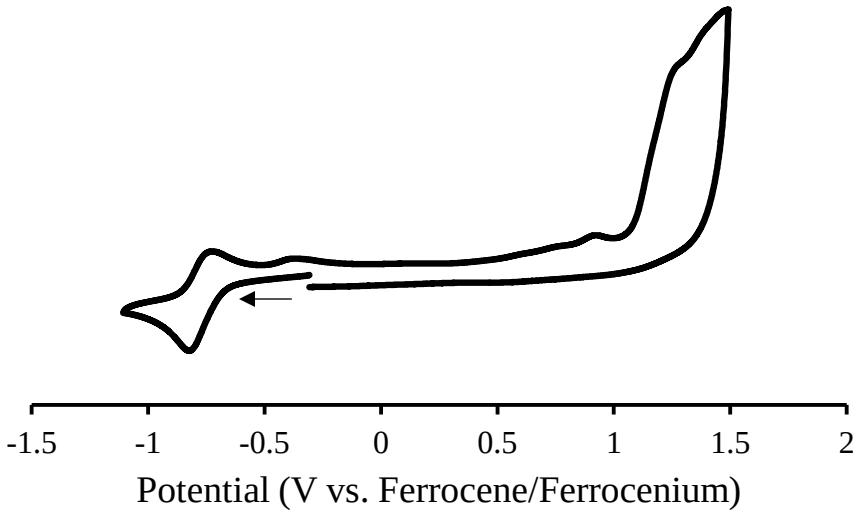

Figure S24. Cyclic voltammograms of complex **13** recorded at 100 mV s^{-1} in 1 mM CH_2Cl_2 solution containing 0.1 M [nBu$_4$N][PF_6] as supporting electrolyte.

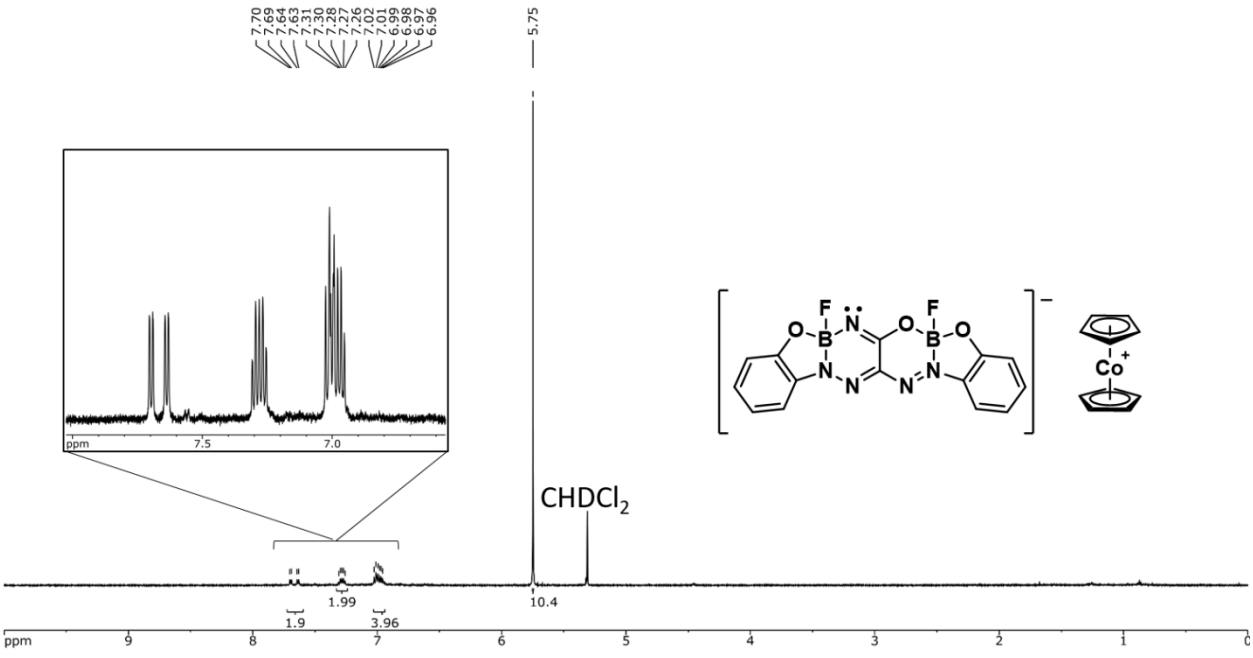

Figure S25. ^{1}H NMR spectrum of **16**$^-$ in CD_2Cl_2.

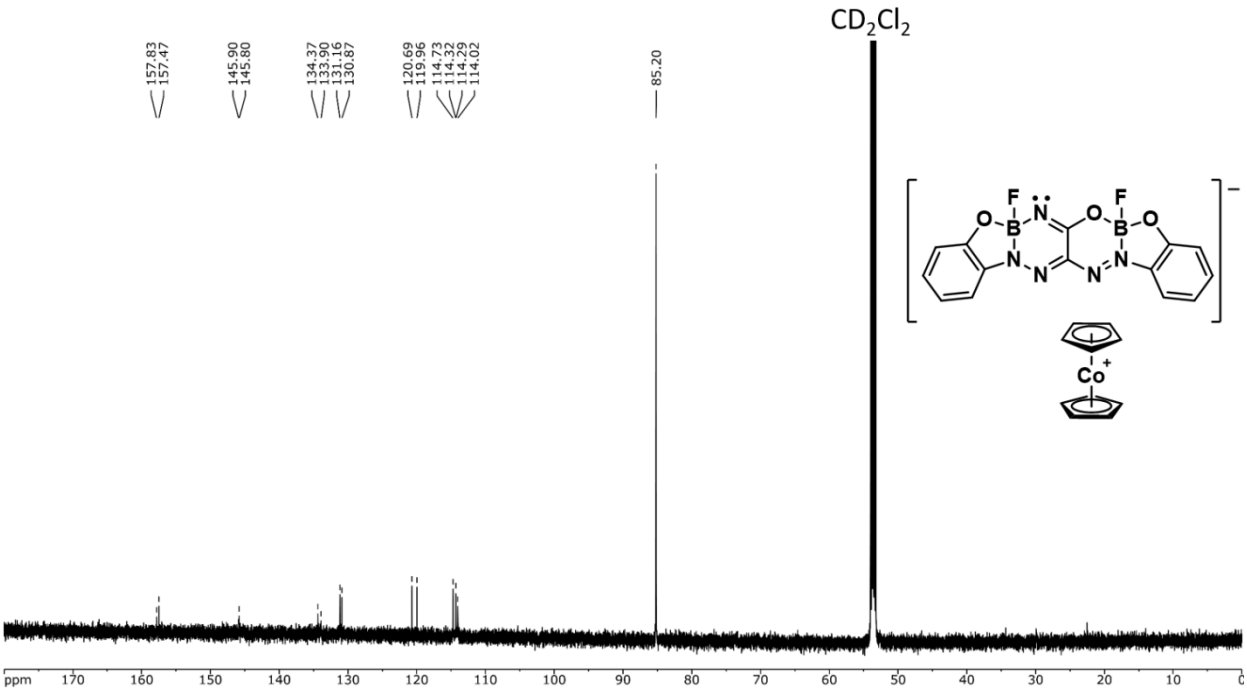

Figure S26. $^{13}C\{^{1}H\}$ NMR spectrum of **16**$^{-}$ in CD_2Cl_2.

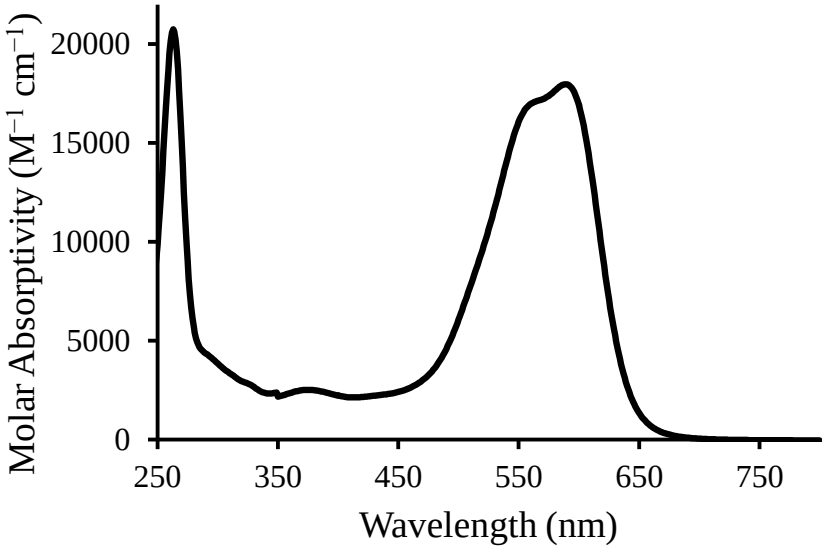

Figure S27. UV-vis absorption spectrum of complex **16**$^{-}$ in CH_2Cl_2.

Table S5. Changes in the total electronic energy, enthalpy and Gibbs free energy for the reactions of **7** to form **8**−**13** and the reaction of **14** to form **15**, in the gas phase and in a toluene solution, calculated using the PBE1PBE density functional and the 6-311+G(d,p) basis set. All values are per mole of the reactant (**7** or **14**).

Reaction	ΔE_e (kJ mol^{-1})	$\Delta H°_{353}$ (kJ mol^{-1})	$\Delta G°_{353}$ (kJ mol^{-1})
Gas phase			
7→**8**	180.7	161.2	91.2
7→**9**	100.7	85.7	47.1
7→**10**	105.9	90.7	53.4
7→**11**	35.8	26.9	2.1
7→**12**	−125.6	−124.4	−76.9
7→**13**	−49.7	−57.3	−54.0
14→**15**	90.5	70.9	−1.9
Toluene solution (polarized continuum model)			
7→**8**	164.8	145.3	75.7
7→**9**	87.4	72.4	34.1
7→**10**	91.7	76.6	39.9
7→**11**	27.4	18.3	−6.2
7→**12**	−133.4	−132.3	−84.2
7→**13**	−64.9	−72.6	−68.6
14→**15**	72.6	52.9	−19.4

Table S6. Frontier-orbital energies and first singlet-singlet electronic excitation energies (ΔE) of complexes **13** and **16**$^-$ in dichloromethane solution calculated with time-dependent density-functional theroy at the PBE1PBE/6-311+G(d,p) level using the SCRF method.

	Orbital energies (eV)					
Compound	**HOMO**	**LUMO**	**Oscillator strength**	ΔE_{calc} **(eV)**	ΔE_{calc} **(nm)**	ΔE_{exp} **(nm)**
13	−6.49	−3.52	*f*=1.03	2.44	508	577
16$^-$	−5.66	−2.78	*f*=1.06	2.40	516	589

Reaction stoichiometries used to compute ΔE_e, $\Delta H°$, and $\Delta G°$.

7 + BF_3 → **8** + 3HF

7 + BF_3 → ½ **9** + 3HF

7 + BF_3 → ½ **10** + 3HF

7 + BF_3 → **11** + 2HF

7 + $2BF_3$ + H_2O → **12** + 3HF

7 + $2BF_3$ + H_2O → **13** + 4HF

14 + BF_3 → **15** + 3HF

# PBE1PBE 6-311+G(d,p) SCRF=(PCM,Solvent=Toluene)
Temperature=353.15

Compound **7** / Optimized geometry

0,1

C	-1.338145	2.674505	0.000000
C	0.060995	2.592382	0.000000
C	0.827022	3.755473	0.000000
C	0.199532	4.991736	0.000000
C	-1.190403	5.071922	0.000000
C	-1.959715	3.913899	0.000000
N	0.607554	1.314706	0.000000
N	1.887252	1.109437	0.000000
C	2.315928	-0.135718	0.000000
C	3.741418	-0.280770	0.000000
N	4.889296	-0.403417	0.000000
O	-2.015987	1.492038	0.000000
N	1.639914	-1.330272	0.000000
N	0.369505	-1.287434	0.000000
C	-0.268958	-2.527007	0.000000
C	0.404712	-3.759547	0.000000
C	-0.300372	-4.943512	0.000000
C	-1.700308	-4.916026	0.000000
C	-2.382720	-3.714018	0.000000
C	-1.679345	-2.508578	0.000000
O	-2.398118	-1.374320	0.000000
H	0.000000	0.488219	0.000000
H	1.907020	3.669400	0.000000
H	0.797535	5.895805	0.000000
H	-1.682226	6.038164	0.000000
H	-3.044743	3.971027	0.000000
H	-2.964836	1.648221	0.000000
H	-3.466307	-3.678220	0.000000
H	-2.259920	-5.845584	0.000000
H	0.226808	-5.890820	0.000000
H	1.488066	-3.748244	0.000000
H	-1.821047	-0.599281	0.000000

# PBE1PBE 6-311+G(d,p) SCRF=(PCM,Solvent=Toluene)
Temperature=353.15

Compound **8** / Optimized geometry

0,1

C	0.327682	2.046580	-1.230335
C	-0.591983	2.260988	-0.184316

```
C    -1.209127    3.480774    0.040633
C    -0.910848    4.509973   -0.840920
C     0.000000    4.310056   -1.885252
C     0.640276    3.091823   -2.087651
N    -0.559487    1.081419    0.564956
N    -0.544847    1.077341    1.849963
C     0.000000    0.000000    2.435296
C     0.000000    0.000000    3.864885
N     0.000000    0.000000    5.018247
O     0.862773    0.812684   -1.250301
B     0.000000    0.000000   -0.376825
O    -0.862773   -0.812684   -1.250301
C    -0.327682   -2.046580   -1.230335
C     0.591983   -2.260988   -0.184316
C     1.209127   -3.480774    0.040633
C     0.910848   -4.509973   -0.840920
C     0.000000   -4.310056   -1.885252
C    -0.640276   -3.091823   -2.087651
N     0.559487   -1.081419    0.564956
N     0.544847   -1.077341    1.849963
H    -1.355864   -2.949056   -2.888653
H    -0.215152   -5.132256   -2.559799
H     1.384174   -5.477305   -0.719292
H     1.893690   -3.613035    0.870418
H    -1.893690    3.613035    0.870418
H    -1.384174    5.477305   -0.719292
H     0.215152    5.132256   -2.559799
H     1.355864    2.949056   -2.888653

# PBE1PBE 6-311+G(d,p) SCRF=(PCM,Solvent=Toluene)
  Temperature=353.15

Compound 9 / Optimized geometry

0,1
B     1.627137    0.378695    0.072504
O     1.722202   -0.605396    1.138390
O    -0.929242    0.028181    1.110874
N     3.144283    0.677343   -0.190132
N     3.599868    1.671095   -0.851315
N     1.097367    1.808158    0.379998
N     1.558815    2.794668   -0.322321
N     3.339786    4.596541   -2.577468
C     2.676549    2.637870   -1.031152
C     3.046530    3.728337   -1.876812
C     3.904235   -0.262135    0.480285
C     3.000120   -0.989586    1.273159
```

C	3.467576	-1.986048	2.118057
H	2.780157	-2.549107	2.737915
C	4.835804	-2.230604	2.128814
H	5.223000	-3.012384	2.773810
C	5.731179	-1.499060	1.335293
H	6.790721	-1.723278	1.378794
C	5.275405	-0.490840	0.501800
H	5.946304	0.097945	-0.112865
C	0.114101	2.162238	1.332017
C	-0.918930	1.263014	1.645999
C	-1.892557	1.649503	2.563564
H	-2.677717	0.942664	2.808957
C	-1.851642	2.904902	3.152143
H	-2.617199	3.186116	3.867421
C	-0.827760	3.795247	2.836478
H	-0.785975	4.772316	3.304096
C	0.151542	3.421875	1.933536
H	0.962816	4.094570	1.681084
B	-1.627107	-0.378712	-0.072503
O	-1.722176	0.605358	-1.138409
O	0.929268	-0.028170	-1.110884
N	-3.144247	-0.677380	0.190127
N	-3.599817	-1.671130	0.851325
N	-1.097315	-1.808170	-0.379978
N	-1.558746	-2.794681	0.322351
N	-3.340351	-4.595963	2.577969
C	-2.676483	-2.637890	1.031177
C	-3.046443	-3.728361	1.876841
C	-3.904211	0.262070	-0.480319
C	-3.000099	0.989521	-1.273198
C	-3.467564	1.985956	-2.118123
H	-2.780148	2.549014	-2.737986
C	-4.835797	2.230488	-2.128901
H	-5.223000	3.012247	-2.773919
C	-5.731167	1.498944	-1.335375
H	-6.790712	1.723141	-1.378893
C	-5.275384	0.490750	-0.501856
H	-5.946279	-0.098035	0.112813
C	-0.114063	-2.162240	-1.332014
C	0.918946	-1.262999	-1.646020
C	1.892542	-1.649463	-2.563628
H	2.677680	-0.942607	-2.809045
C	1.851625	-2.904857	-3.152217
H	2.617160	-3.186051	-3.867527
C	0.827770	-3.795222	-2.836521
H	0.785984	-4.772288	-3.304146
C	-0.151507	-3.421872	-1.933543

```
H    -0.962764   -4.094580   -1.681070

# PBE1PBE 6-311+G(d,p) SCRF=(PCM,Solvent=Toluene)
  Temperature=353.15

Compound 10 / Optimized geometry

0,1
B    -1.700471    0.509194   -0.107182
B     1.700472    0.509177    0.107217
N    -3.220933    0.246358    0.183959
N    -3.738638   -0.855451    0.570755
N    -1.312952   -0.829184   -0.795996
N    -1.836592   -1.943572   -0.377926
N     3.220923    0.246339   -0.183970
N     3.738618   -0.855465   -0.570794
N     1.312954   -0.829213    0.795993
N     1.836581   -1.943597    0.377897
N    -3.706508   -4.157069    1.395973
N     3.706311   -4.157078   -1.396170
O    -1.770810    1.690750   -0.944689
O     0.950576    0.792131   -1.082173
O     1.770835    1.690698    0.944773
O    -0.950598    0.792083    1.082231
C    -2.905957   -1.906988    0.414555
C     2.905935   -1.907003   -0.414598
C    -3.349152   -3.156814    0.946475
C     3.349126   -3.156820   -0.946541
C    -3.925915    1.376585   -0.187112
C    -3.009218    2.192802   -0.874748
C    -3.439291    3.385626   -1.440766
H    -2.744562    4.019428   -1.978713
C    -4.775905    3.729629   -1.282136
H    -5.130005    4.663939   -1.705087
C    -5.682752    2.908083   -0.596173
H    -6.717298    3.216603   -0.499999
C    -5.269285    1.706403   -0.046137
H    -5.950694    1.045553    0.476911
C    -0.464071   -0.946658   -1.921737
C     0.662502   -0.115204   -2.037872
C     1.460938   -0.219714   -3.174454
H     2.315594    0.441958   -3.263738
C     1.170606   -1.154704   -4.157406
H     1.805650   -1.224609   -5.034037
C     0.071517   -1.999899   -4.022080
H    -0.156458   -2.730989   -4.789169
C    -0.745854   -1.889923   -2.910945
```

```
H    -1.619711   -2.520746   -2.795251
C     3.925915    1.376559    0.187113
C     3.009239    2.192755    0.874800
C     3.439330    3.385567    1.440834
H     2.744620    4.019355    1.978819
C     4.775938    3.729575    1.282168
H     5.130046    4.663878    1.705131
C     5.682764    2.908049    0.596153
H     6.717306    3.216575    0.499953
C     5.269280    1.706383    0.046100
H     5.950674    1.045550   -0.476989
C     0.464084   -0.946704    1.921745
C    -0.662498   -0.115266    2.037904
C    -1.460921   -0.219804    3.174494
H    -2.315586    0.441854    3.263788
C    -1.170564   -1.154799    4.157433
H    -1.805598   -1.224728    5.034068
C    -0.071461   -1.999974    4.022086
H     0.156540   -2.731065    4.789164
C     0.745894   -1.889972    2.910940
H     1.619758   -2.520783    2.795234
```

```
# PBE1PBE 6-311+G(d,p) SCRF=(PCM,Solvent=Toluene)
  Temperature=353.15
```

Compound **11** / Optimized geometry

```
0,1
C     3.137551   -0.122566   -0.671405
C     2.016730   -0.550157    0.083456
C     1.991622   -1.856224    0.598267
C     3.024673   -2.733914    0.351399
C     4.111296   -2.320629   -0.423563
C     4.163946   -1.034388   -0.923588
N     0.919135    0.285088    0.344763
N     1.068154    1.559894    0.132999
C     0.010362    2.380472    0.146223
C     0.296764    3.773332    0.017687
N     0.531390    4.899111   -0.070755
O     3.274001    1.109968   -1.172111
N    -1.277329    2.014651    0.056429
N    -1.455260    0.766106    0.281011
B    -0.434690   -0.188805    0.950403
F    -0.383692   -0.007635    2.320339
O    -0.946691   -1.489976    0.563143
C    -2.186571   -1.324952    0.069419
C    -3.064051   -2.334857   -0.292145
```

```
C    -4.298161   -1.958970   -0.811425
C    -4.655052   -0.614833   -0.986207
C    -3.777088    0.400843   -0.644272
C    -2.552142    0.021371   -0.108384
H     1.146301   -2.174992    1.194231
H    -2.789345   -3.375206   -0.166151
H    -5.006136   -2.731867   -1.091123
H    -5.627944   -0.368805   -1.395566
H    -4.024131    1.447551   -0.777216
H     5.006100   -0.688804   -1.512383
H     4.926435   -3.006616   -0.627469
H     2.988985   -3.736377    0.760911
H     2.566033    1.666776   -0.792450

# PBE1PBE 6-311+G(d,p) SCRF=(PCM,Solvent=Toluene)
  Temperature=353.15

Compound 12 / Optimized geometry

0,1
B     2.183982   -1.818880   -0.324651
B    -2.576550   -1.293297    0.467259
F     2.794967   -2.485348    0.723446
F     2.827831   -2.049986   -1.524950
F    -2.487766   -1.608838    1.807733
O     2.353382    2.674671    0.192720
H     1.568960    2.088756    0.232222
O    -3.910545   -1.414227   -0.070854
O    -1.522043   -2.021486   -0.265747
N     2.178547   -0.245079   -0.019915
N     1.104651    0.430554    0.159909
N    -2.279097    0.236072    0.259781
N    -1.128772    0.766826    0.199260
N     0.717416   -2.254473   -0.429989
H     0.526691   -3.222647   -0.666672
C    -0.111283   -0.125689    0.138254
C    -0.327416   -1.524143   -0.168996
C     3.391923    0.475786    0.020751
C     3.435242    1.892063    0.116319
C     4.677329    2.529749    0.124216
H     4.679379    3.611778    0.192972
C     5.851827    1.807817    0.053652
H     6.802831    2.329496    0.065680
C     5.814804    0.414770   -0.027109
H     6.731978   -0.160113   -0.075331
C     4.600524   -0.237330   -0.044065
H     4.577646   -1.315961   -0.101848
```

```
C    -3.494579    0.861251    0.040302
C    -4.427837   -0.174969   -0.160851
C    -5.745825    0.135536   -0.456307
H    -6.472309   -0.651806   -0.617670
C    -6.091767    1.480691   -0.537000
H    -7.119982    1.743770   -0.762057
C    -5.156514    2.504437   -0.339137
H    -5.470922    3.539110   -0.410808
C    -3.833794    2.205064   -0.052759
H    -3.088105    2.976891    0.098523
```

```
# PBE1PBE 6-311+G(d,p) SCRF=(PCM,Solvent=Toluene)
  Temperature=353.15
```

Compound **13** / Optimized geometry

```
0,1
B     2.385130   -1.336210    0.126747
B    -2.347129   -1.308270    0.106778
F     2.508466   -1.986910    1.348581
F    -2.352928   -1.985475    1.309615
O     3.623565   -1.384274   -0.634046
O    -3.599302   -1.391877   -0.609392
O    -1.148607   -1.700069   -0.658618
N     2.208091    0.206168    0.355151
N     1.127780    0.841489    0.551741
N    -2.214067    0.234732    0.352357
N    -1.133013    0.867997    0.540447
N     1.103261   -1.764396   -0.569938
H     1.015293   -2.637253   -1.078303
C    -0.008086    0.128070    0.398521
C    -0.027729   -1.174380   -0.262042
C     3.454729    0.784433    0.150357
C     4.249229   -0.206926   -0.454656
C     5.546942    0.093318   -0.840370
H     6.167056   -0.659773   -1.311917
C     6.014452    1.381220   -0.598637
H     7.030212    1.632223   -0.885780
C     5.215604    2.361386    0.002164
H     5.619790    3.352379    0.173479
C     3.912107    2.074585    0.379739
H     3.268659    2.816107    0.838917
C    -3.468428    0.791289    0.148994
C    -4.248116   -0.225130   -0.434961
C    -5.557299    0.040044   -0.804458
H    -6.166528   -0.732205   -1.258712
C    -6.049423    1.321033   -0.572860
```

```
H    -7.073914    1.546115   -0.850262
C    -5.265062    2.326746    0.004291
H    -5.689201    3.310653    0.167806
C    -3.950883    2.074028    0.368871
H    -3.319038    2.835147    0.811793

# PBE1PBE 6-311+G(d,p) SCRF=(PCM,Solvent=Toluene)
  Temperature=353.15

Compound 14 / Optimized geometry

0,1
C     3.387406    0.992871    0.977377
C     2.588139    0.231097    0.117467
C     3.091206   -0.955283   -0.441124
C     4.402363   -1.325808   -0.141871
C     5.192402   -0.573239    0.717147
C     4.676334    0.589142    1.282301
N     1.261979    0.629391   -0.181077
N     1.122066    1.883518   -0.154276
C    -0.150483    2.389086   -0.283820
C    -0.185718    3.817377   -0.401786
N    -0.207433    4.966778   -0.509229
C     2.285114   -1.840673   -1.347882
O     1.676476   -2.924912   -0.637495
N    -1.330873    1.820083   -0.209617
N    -1.478275    0.542473   -0.112405
C    -2.767927    0.009546    0.068976
C    -3.892720    0.825885   -0.050169
C    -5.155660    0.290980    0.148564
C    -5.306148   -1.055483    0.462844
C    -4.179908   -1.861462    0.573978
C    -2.899227   -1.351130    0.388049
C    -1.695694   -2.232986    0.548940
O    -0.882656   -2.108811   -0.599685
H    -0.681943   -0.095611   -0.223851
H    -3.762452    1.872184   -0.296536
H    -6.026270    0.930516    0.050233
H    -6.293993   -1.477480    0.611747
H    -4.290230   -2.915504    0.810420
H     4.814237   -2.218429   -0.606084
H     6.206373   -0.887933    0.939399
H     5.281043    1.183335    1.959196
H     2.972610    1.897797    1.405453
H    -0.030440   -2.555573   -0.450820
H    -1.136878   -1.933558    1.450310
H    -2.026412   -3.268108    0.697884
```

```
H     1.464525   -1.296882   -1.814370
H     2.928360   -2.241543   -2.139021
H     2.321798   -3.318660   -0.044242

# PBE1PBE 6-311+G(d,p) SCRF=(PCM,Solvent=Toluene)
  Temperature=353.15

Compound 15 / Optimized geometry

0,1
B     0.000037   -0.336692    0.000062
O    -0.181540   -1.100147   -1.196879
O     0.181672   -1.099981    1.197097
N    -1.231434    0.611572    0.107399
N    -1.201660    1.886079    0.085106
N     1.231429    0.611652   -0.107383
N     1.201585    1.886156   -0.085105
N    -0.000445    5.057917    0.000089
C    -0.000057    2.476449    0.000007
C    -0.000096    3.903644    0.000020
C    -2.488008   -0.029378    0.069899
C    -2.530304   -1.299397   -0.517263
C    -3.758868   -1.954293   -0.556333
H    -3.818552   -2.936374   -1.016959
C    -4.902145   -1.364418   -0.036667
H    -5.848752   -1.892280   -0.081028
C    -4.838465   -0.093667    0.534985
H    -5.730997    0.367004    0.943615
C    -3.631396    0.578931    0.588698
H    -3.550921    1.563154    1.034857
C    -1.302381   -1.948128   -1.116114
H    -1.071132   -2.848764   -0.526580
H    -1.536217   -2.279958   -2.132411
C     2.488028   -0.029242   -0.069952
C     2.530426   -1.299194    0.517351
C     3.759002   -1.954068    0.556301
H     3.818774   -2.936109    1.017004
C     4.902199   -1.364225    0.036410
H     5.848815   -1.892075    0.080686
C     4.838420   -0.093533   -0.535357
H     5.730888    0.367111   -0.944161
C     3.631326    0.579031   -0.588976
H     3.550760    1.563200   -1.035240
C     1.302616   -1.947854    1.116519
H     1.071419   -2.848728    0.527334
H     1.536580   -2.279279    2.132925
```

PBE1PBE 6-311+G(d,p) SCRF=(PCM,Solvent=Dichloromethane)

Compound **13** / Optimized geometry in a CH2Cl2 solution, T = 298.15 K

0,1

B	2.384224	-1.334376	0.123754
B	-2.346392	-1.305692	0.103232
F	2.513945	-1.985812	1.351204
F	-2.361593	-1.989152	1.308473
O	3.624383	-1.384797	-0.633353
O	-3.598066	-1.390898	-0.613656
O	-1.149162	-1.703410	-0.655319
N	2.208447	0.205645	0.354730
N	1.127235	0.839656	0.551356
N	-2.214508	0.233497	0.353941
N	-1.132306	0.865285	0.541522
N	1.103279	-1.768768	-0.565686
H	1.019334	-2.639115	-1.080017
C	-0.007912	0.125836	0.398189
C	-0.026595	-1.177304	-0.261295
C	3.454770	0.785014	0.149926
C	4.250328	-0.205059	-0.455066
C	5.547542	0.094815	-0.841632
H	6.168751	-0.656500	-1.314748
C	6.014666	1.383454	-0.599949
H	7.029891	1.635142	-0.888026
C	5.215179	2.362894	0.001587
H	5.618611	3.354179	0.172683
C	3.911669	2.075595	0.379652
H	3.269685	2.817984	0.839388
C	-3.468720	0.791320	0.150464
C	-4.248635	-0.222041	-0.437511
C	-5.556659	0.043196	-0.808936
H	-6.166383	-0.726112	-1.267672
C	-6.049110	1.324216	-0.574335
H	-7.072786	1.550494	-0.853322
C	-5.265082	2.327565	0.007492
H	-5.688928	3.311170	0.173171
C	-3.951283	2.073666	0.373704
H	-3.321716	2.834410	0.820365

PBE1PBE 6-311+G(d,p) SCRF=(PCM,Solvent=Dichloromethane)

Compound **16**$^{-}$ / Optimized geometry in a CH2Cl2 solution, T = 298.15 K

0,1

B	2.323919	-1.342081	0.129995
B	-2.300714	-1.311908	0.036186
F	2.504349	-1.927498	1.412011
F	-2.339330	-2.013645	1.252958
O	3.619594	-1.410295	-0.597200
O	-3.593570	-1.390732	-0.649896
O	-1.151250	-1.685585	-0.739451
N	2.204764	0.214572	0.330991
N	1.121906	0.863949	0.500872
N	-2.202028	0.220056	0.329378
N	-1.115243	0.865147	0.504368
N	1.107758	-1.858968	-0.528442
C	0.000025	0.130903	0.347922
C	0.036065	-1.223452	-0.287823
C	3.454167	0.777511	0.126748
C	4.249485	-0.242533	-0.436158
C	5.560035	0.039315	-0.802772
H	6.182481	-0.731364	-1.243269
C	6.041017	1.328596	-0.588573
H	7.065292	1.559252	-0.863496
C	5.241937	2.333039	-0.031946
H	5.652143	3.325198	0.119565
C	3.926021	2.067182	0.326975
H	3.283365	2.830255	0.751570
C	-3.459925	0.775067	0.150865
C	-4.246082	-0.233981	-0.440112
C	-5.564092	0.031827	-0.778658
H	-6.177547	-0.734065	-1.239329
C	-6.064688	1.305979	-0.514324
H	-7.095468	1.528511	-0.770304
C	-5.275682	2.302245	0.067073
H	-5.699606	3.281891	0.257071
C	-3.950491	2.047316	0.403487
H	-3.316883	2.806048	0.848557

References:

[1] J. B. Gilroy, P. O. Otieno, M. J. Ferguson, R. McDonald, and R. G. Hicks, *Inorg. Chem.*, **2008,** *47*, 1279−1286.

[2] V. P. Fadeeva, V. D. Tikhova, and O. N. Nikulicheva, *J. Anal. Chem.*, **2008,** *63*, 1094−1106.

[3] L.-L. Liu, G.-Q. He, Y.-H. Wang, and S.-Q. Hu, *RSC Adv.*, **2015,** *5*, 101416−101426.

[4] Bruker-Nonius, SAINT version 2013.8, 2013, Bruker-AXS, Madison, WI 53711, USA.

[5] Bruker-Nonius, SADABS version 2012.1, 2012, Bruker-AXS, Madison, WI 53711, USA.

[6] Bruker-Nonius, TWINABS version 2012.1, 2012, Bruker-AXS, Madison, WI 53711, USA.

[7] G. M. Sheldrick, *Acta Cryst.*, **2015,** *A71*, 3−8.

[8] A. L. Spek, *Acta Cryst.*, **2015,** *C71*, 9−19.

[9] G. M. Sheldrick, *Acta Cryst.*, **2015,** *C71*, 3−8.